

2F

PNL-3070

UC-70

Assessment of Effectiveness of
Geologic Isolation Systems

**Comparison of INTERA and
WISAP Consequence Model
Application**

C. R. Cole
F. W. Bond

January 1980

Prepared for the
Office of Nuclear Waste Isolation
under its Contract with the
U.S. Department of Energy

Pacific Northwest Laboratory
Operated for the U.S. Department of Energy
by Battelle Memorial Institute

 **Battelle**

PNL-3070

NOTICE

This report was prepared as an account of work sponsored by the United States Government. Neither the United States nor the Department of Energy, nor any of their employees, nor any of their contractors, subcontractors, or their employees, makes any warranty, express or implied, or assumes any legal liability or responsibility for the accuracy, completeness or usefulness of any information, apparatus, product or process disclosed, or represents that its use would not infringe privately owned rights.

The views, opinions and conclusions contained in this report are those of the contractor and do not necessarily represent those of the United States Government or the United States Department of Energy.

PACIFIC NORTHWEST LABORATORY
operated by
BATTELLE
for the
UNITED STATES DEPARTMENT OF ENERGY
Under Contract EY-76-C-06-1830

Printed in the United States of America
Available from
National Technical Information Service
United States Department of Commerce
5285 Port Royal Road
Springfield, Virginia 22151

Price: Printed Copy \$____*; Microfiche \$3.00

*Pages	NTIS Selling Price
001-025	\$4.00
026-050	\$4.50
051-075	\$5.25
076-100	\$6.00
101-125	\$6.50
126-150	\$7.25
151-175	\$8.00
176-200	\$9.00
201-225	\$9.25
226-250	\$9.50
251-275	\$10.75
276-300	\$11.00

3 3679 00053 6674

Assessment of Effectiveness of
Geologic Isolation Systems

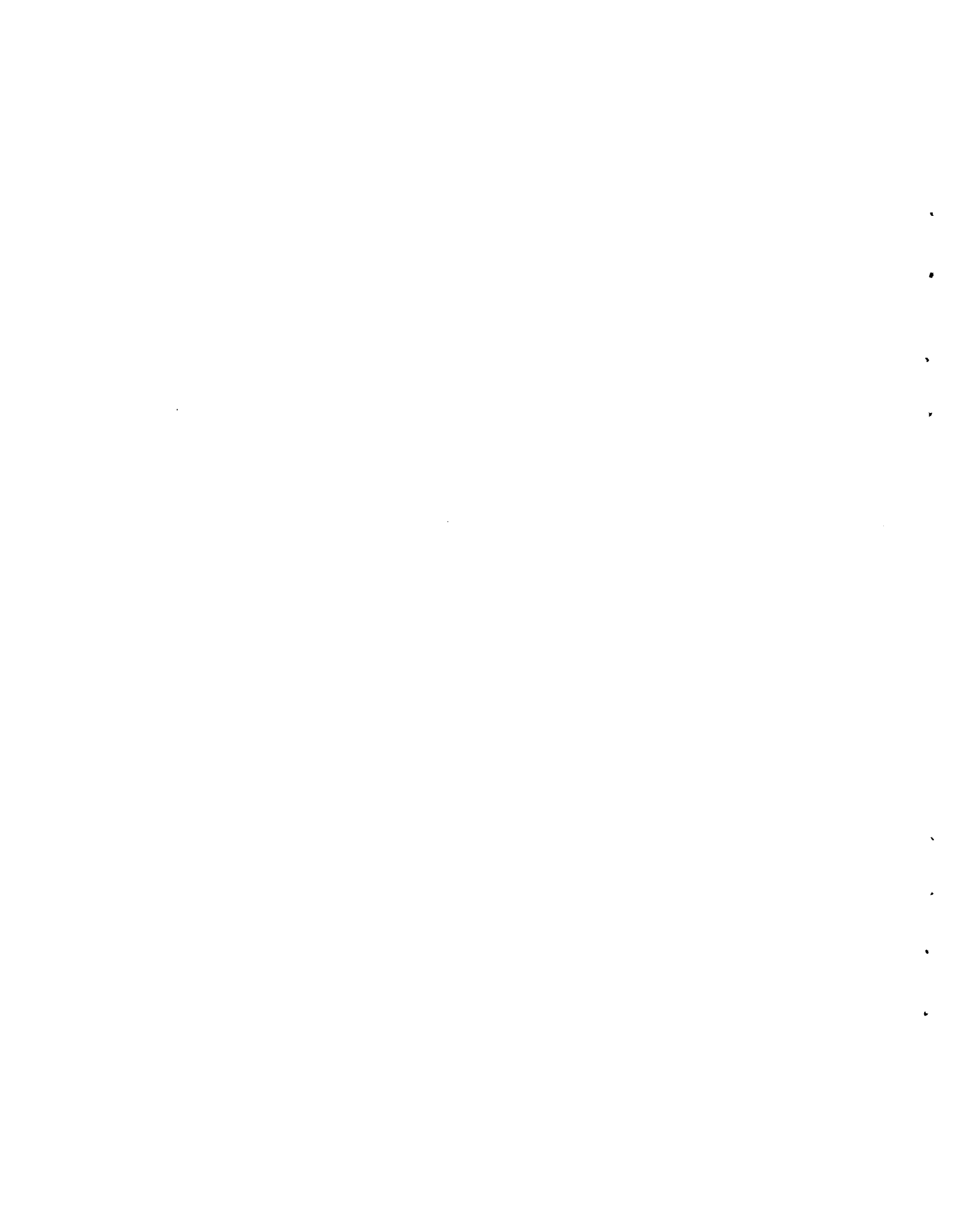
COMPARISON OF INTERA AND WISAP CONSEQUENCE
MODEL APPLICATION

C. R. Cole
F. W. Bond

January 1980

Prepared for the
Office of Nuclear Waste Isolation
under its Contract with the
U.S. Department of Energy
EY-76-C-06-1830

Pacific Northwest Laboratory
Richland, Washington 99352



SUMMARY

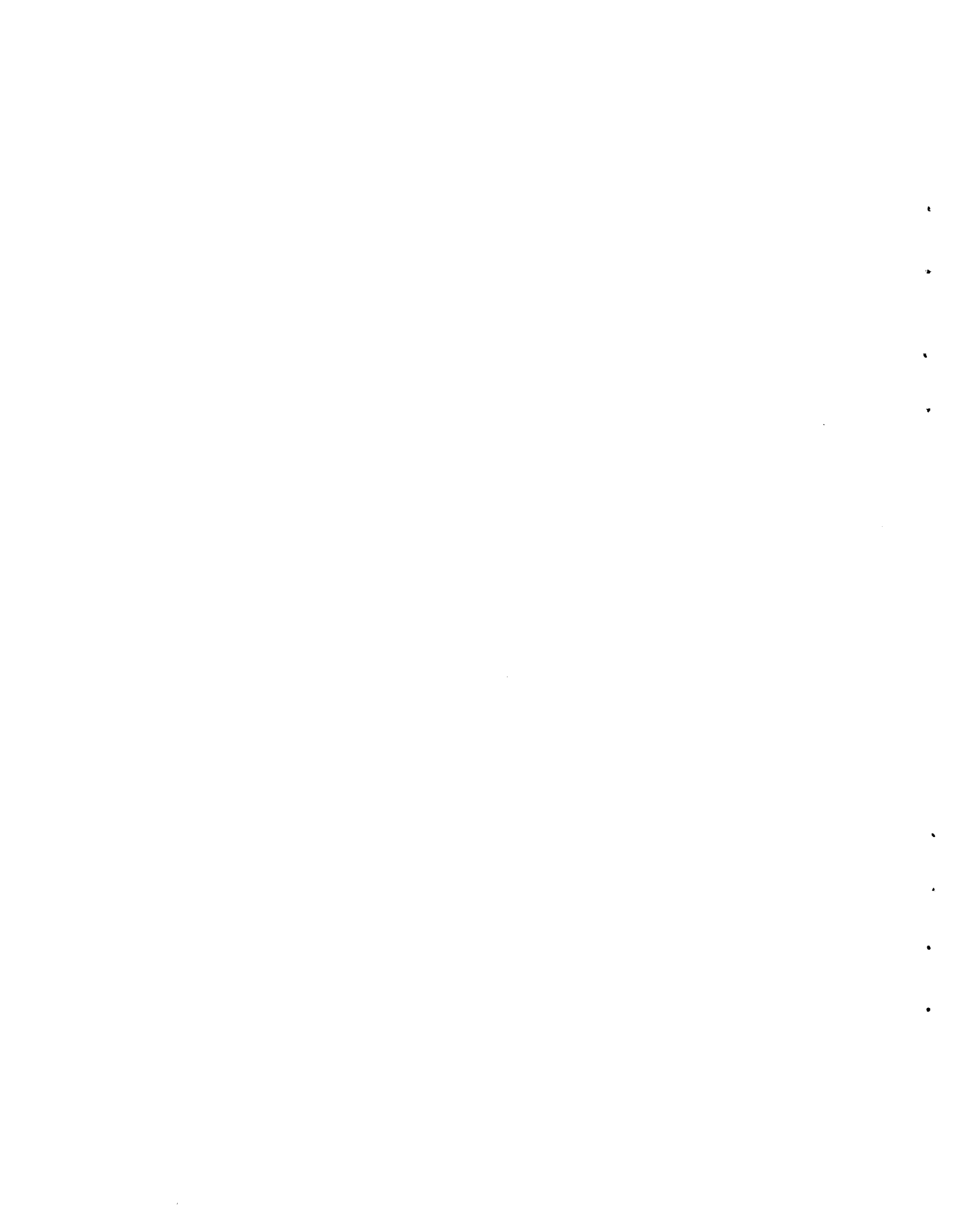
The Waste Isolation Safety Assessment Program (WISAP) is being conducted to develop, for the Office of Nuclear Waste Isolation (ONWI), the methodology necessary to perform long-term safety assessments of deep geologic repositories. The Waste Isolation Pilot Plant (WIPP) program is developing a nuclear waste storage facility and is performing assessments of that site. WISAP and WIPP have similar, though independent, methodologies for assessing the consequences of a repository breach subsequent to closure. Intera Environmental Consultants are under contract to Sandia Laboratories to conduct the hydrologic and transport modeling for the WIPP Site Release Consequence Analysis (WIPP EIS/ER 1978). To provide a mutual benchmark check of the radionuclide and ground-water transport models of these two programs, ONWI has requested WISAP to perform a release consequence analysis based on the WIPP site, utilizing the same data and conceptual model which the WIPP program used for its environmental assessments. Therefore, only a portion of the WISAP methodology was used; specifically, only WISAP geotransport models were exercised. The other important parts of WISAP assessment methodology were not used, so that WISAP did not develop the scenario nor did WISAP interpret the field data to develop the conceptual model of the geohydrology of the WIPP site.

This report presents the results of the comparative assessment. Although the different models required slightly different input parameters, the results of the hydrologic simulations show a very close correspondence between the WISAP and WIPP predictions. This was as expected, since the various hydrologic codes available essentially utilize and solve the same basic flow equations. In addition, this report presents the results of the WISAP radionuclide transport model simulations. These results will provide the basis for comparison with WIPP results when these become available.



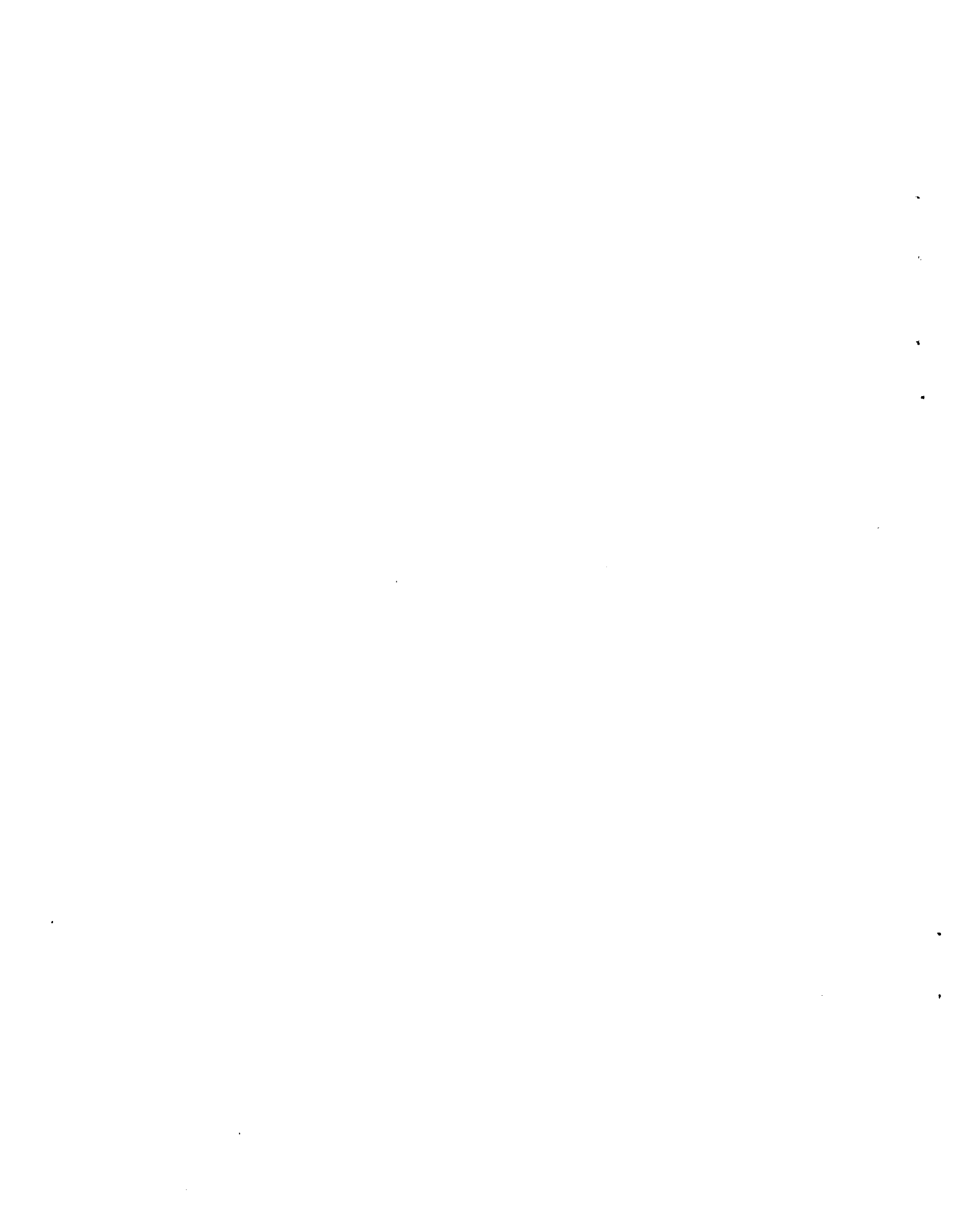
ACKNOWLEDGMENTS

This research was supported by the Waste Isolation Safety Assessment Program (WISAP) conducted by Pacific Northwest Laboratory. This program was sponsored by the Office of Nuclear Waste Isolation managed by Battelle Memorial Institute for the Department of Energy under Contract EY-76-C-06-1830. On 1 October 1979 WISAP was divided into two programs with separate areas of concern: the Assessment of Effectiveness of Geologic Isolation Systems (AEGIS) Program and the Waste/Rock Interaction Technology (WRIT) Program. This report was issued by AEGIS.



CONTENTS

SUMMARY	iii
ACKNOWLEDGMENTS.	v
FIGURES	ix
TABLES	xiii
INTRODUCTION	1
HYDROLOGIC MODELING	2
INTERPRETATION OF THE DATA	2
WISAP HYDROLOGIC MODEL RESULTS.	12
CONCLUSIONS ON WISAP AND INTERA HYDROLOGIC MODELING COMPARISON.	12
TRANSPORT MODELING	30
TRANSPORT MODEL RESULTS	33
TRANSPORT MODELING CONCLUSIONS	33
REFERENCES.	55



FIGURES

1	Geologic Section of the Los Medanos Area.	3
2	Rustler Aquifer Hydraulic Conductivity Distribution Used in the Intera and WISAP Modeling of the WIPP Site	4
3	Shallow Dissolution Zone Hydraulic Conductivity Distribution Used in the Intera and WISAP Modeling of the WIPP Site	5
4	Delaware Mountain Group Hydraulic Conductivity Distribution Used in the Intera and WISAP Modeling of the WIPP Site	6
5	Capitan Aquifer Hydraulic Conductivity Distribution Used in the Intera and WISAP Modeling of the WIPP Site	7
6	Cross Section of Capitan Reef Area	8
7	WISAP Hydraulic Conductivity Distribution Used to Model the Delaware Mountain-Capitan Aquifer Group	9
8	Rustler Formation Interpreted or Measured Hydraulic Potentials	10
9	Delaware Mountain Group and Capitan Interpreted or Measured Hydraulic Potentials	11
10	Rustler Formation Hydraulic Potentials Calculated by the Intera Model	13
11	Delaware Mountain Group and Capitan Hydraulic Potentials Calculated by the Intera Model	14
12	Diagram of the Nodal System WISAP Used to Model the Rustler Aquifer	15
13	Diagram of the Nodal System WISAP Used to Model the Delaware Mountain-Capitan Aquifer System	16
14	Plot Showing the Comparison Between the WISAP VTT Model Predicted Potentials for the Rustler and the Measured or Interpreted Potentials	20
15	Plot Showing the Comparison Between the WISAP VTT Model Predicted Potentials for the Delaware Mountain-Capitan and the Measured or Interpreted Potentials	21

16	Plot Showing the Comparison Between the WIPP Intra Model Predicted Potentials for the Rustler and Measured or Interpreted Potentials	22
17	Plot Showing the Comparison Between the Intra Model Predicted Potentials for the Delaware Mountain-Capitan and the Measured or Interpreted Potentials	23
18	Plot Showing the Comparison Between the WISAP VTT Model Predicted Potentials for the Rustler and the Intra Model Predicted Potentials	25
19	Plot Showing the Comparison Between the WISAP VTT Model Predicted Potentials for the Delaware Mountain-Capitan and the Intra Model Predicted Potentials	26
20	Intra Predicted Potentials and the Associated Streamlines from the WIPP Site	27
21	WISAP Predicted Malaga Bend Arrival Curve for Tc-99	34
22	WISAP Predicted Malaga Bend Arrival Curve for I-129	35
23	WISAP Predicted Malaga Bend Arrival Curve for Cs-135	36
24	WISAP Predicted Alaga Bend Arrival Curve for Actinide Chain 1	37
25	WISAP Predicted Malaga Bend Arrival Curve for Actinide Chain 1	38
26	WISAP Predicted Malaga Bend Arrival for Actinide Chain 1	39
27	WISAP Predicted Malaga Bend Arrival for Actinide Chain 1	40
28	WISAP Predicted Malaga Bend Arrival for Actinide Chain 2	41
29	WISAP Predicted Malaga Bend Arrival for Actinide Chain 2	42
30	WISAP Predicted Malaga Bend Arrival for Actinide Chain 3	43
31	WISAP Predicted Malaga Bend Arrival for Actinide Chain 3	44

32	WISAP Predicted Malaga Bend Arrival for Actinide Chain 3	45
33	WISAP Predicted Malaga Bend Arrival for Actinide Chain 3	46
34	WISAP Predicted Malaga Bend Arrival for Actinide Chain 4	47
35	WISAP Predicted Malaga Bend Arrival for Actinide Chain 4	48



TABLES

1	WISAP VTT Model Predicted Travel Time for the Five Streamlines Shown in Figure 12.	17
2	WISAP Transmissivity Distribution Used to Model the Rustler and Delaware Mountain-Capitan Aquifer System	18
3	Node by Node Comparison Between WISAP VTT Model Predicted Potential Distributions in the 2 Aquifers and the Measured or Interpreted Potentiometric Distribution	19
4	Node by Node Comparison Between the Intera Model Predicted Potential Distributions in the 2 Aquifers and the Measured or Interpreted Potential Distributions	28
5	Predicted Travel Times for the Five Streamlines Which Were Derived from the Intera Model Potentiometric Distribution in Figure 20 and the Hydraulic Conductivity Distribution Used in the Intera Model and Shown in Figure 2	29
6	Comparison Between the WISAP and Intera Travel Time Results	29
7	Characteristics of the One Dimensional Flow Tube Used by Intera to Simulate the Transport from WIPP to Malaga Bend	30
8	WIPP Repository Inventory at 1,000 yr, for the Modeled Nuclides Along With the Half Life and Kd Values Used in the Intera and WISAP Transport Model	32
9	Summary of the WISAP Transport Model Results for Malaga Bend Arrival	49



INTRODUCTION

Intera Environmental Consultants are under contract to Sandia Laboratories to conduct the hydrologic and transport modeling for the WIPP site release consequence analysis (WIPP EIS/ER 1978). To provide a mutual benchmark check of the ground-water and radionuclide transport models of the WIPP and WISAP methodologies, ONWI requested WISAP to perform a release consequence modeling of the WIPP site, using the data and conceptual model provided by the WIPP program. Therefore, only a portion of the WISAP methodology was used. This report presents the WISAP results of the hydrologic modeling and the transport modeling for the WIPP release scenario No. 1 (WIPP EIS/ER 1978).

HYDROLOGIC MODELING

PNL performed the hydrologic modeling by using, as nearly as possible, the same input parameters and the same geohydrologic interpretation made by Intera as reported in WIPP EIS/ER (1978). This geohydrologic interpretation was based only on geohydrologic data collected prior to January 1, 1978.

INTERPRETATION OF THE DATA

A cross-section plot of the geologic layers above and below the proposed repository is shown in Figure 1. Intera modeled the flow in four different geologic units:

1. Rustler (upper aquifer--Figure 2)
2. Shallow dissolution zone (Figure 3)
3. Delaware Mountain Group (below the salt layers Figure 4)
4. Capitan (Figure 5).

Intera concluded that the "travel time for the waste from the repository to either the shallow dissolution zone or the Capitan aquifer would be very long and of little concern" (WIPP EIS/ER 1978); therefore, they only studied flow in the Delaware Mountain Group and the Rustler aquifer.

WISAP deviated slightly from Intera in the modeling of the Delaware Mountain and Capitan. Based on the cross-section plot (Powers et al. 1978) shown in Figure 6 and the hydraulic conductivity distributions for the Delaware Mountain and Capitan shown in Figures 4 and 5, WISAP modeled these as one horizontal layer with the hydraulic conductivity distribution shown in Figure 7 instead of two separate layers in vertical communication.

The measured hydraulic potential distributions^(a) for the Rustler Formation and the Delaware Mountain Group-Capitan aquifer are shown in Figures 8 and 9, respectively. All model-predicted potential distribution results were

(a) It should be noted that the data on potentials are measured at discrete point (wells) and these potential distributions are interpreted from these discrete data by a geohydrologist.

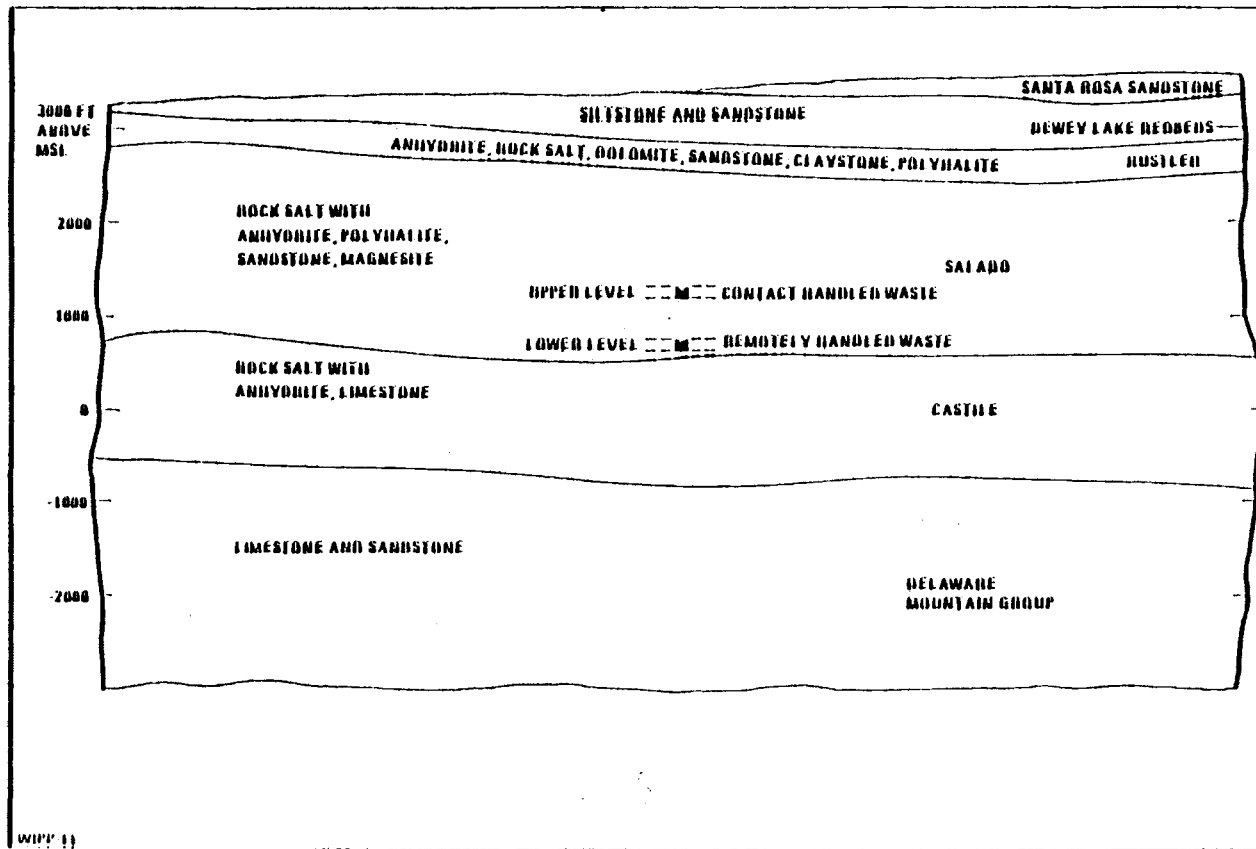


FIGURE 1. Geologic Section of the Los Medanos Area (WIPP EIS/ER 1978)

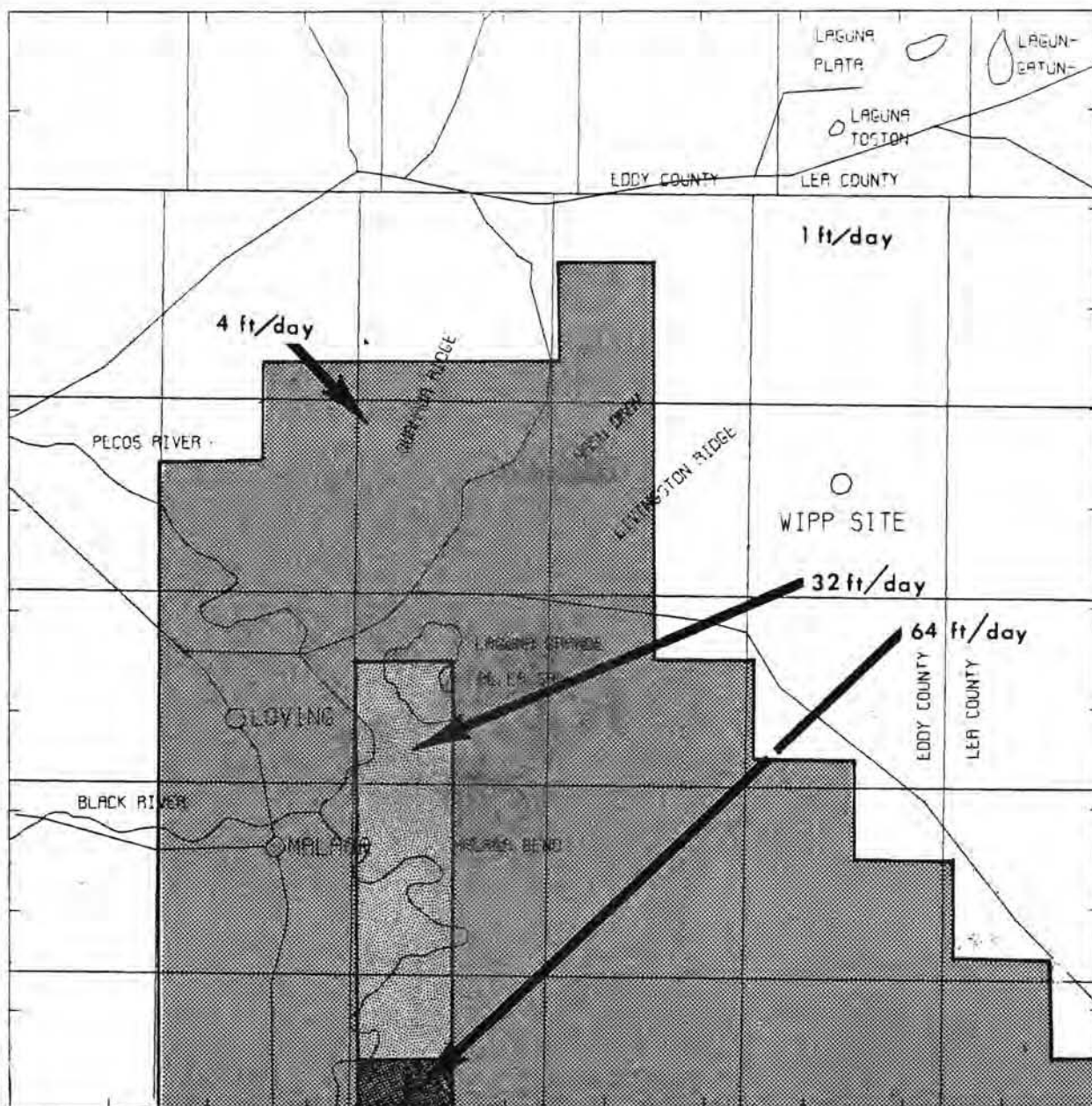


FIGURE 2. Rustler Aquifer Hydraulic Conductivity Distribution (WIPP EIS/ER 1978) Used in the Intera and WISAP Modeling of the WIPP Site

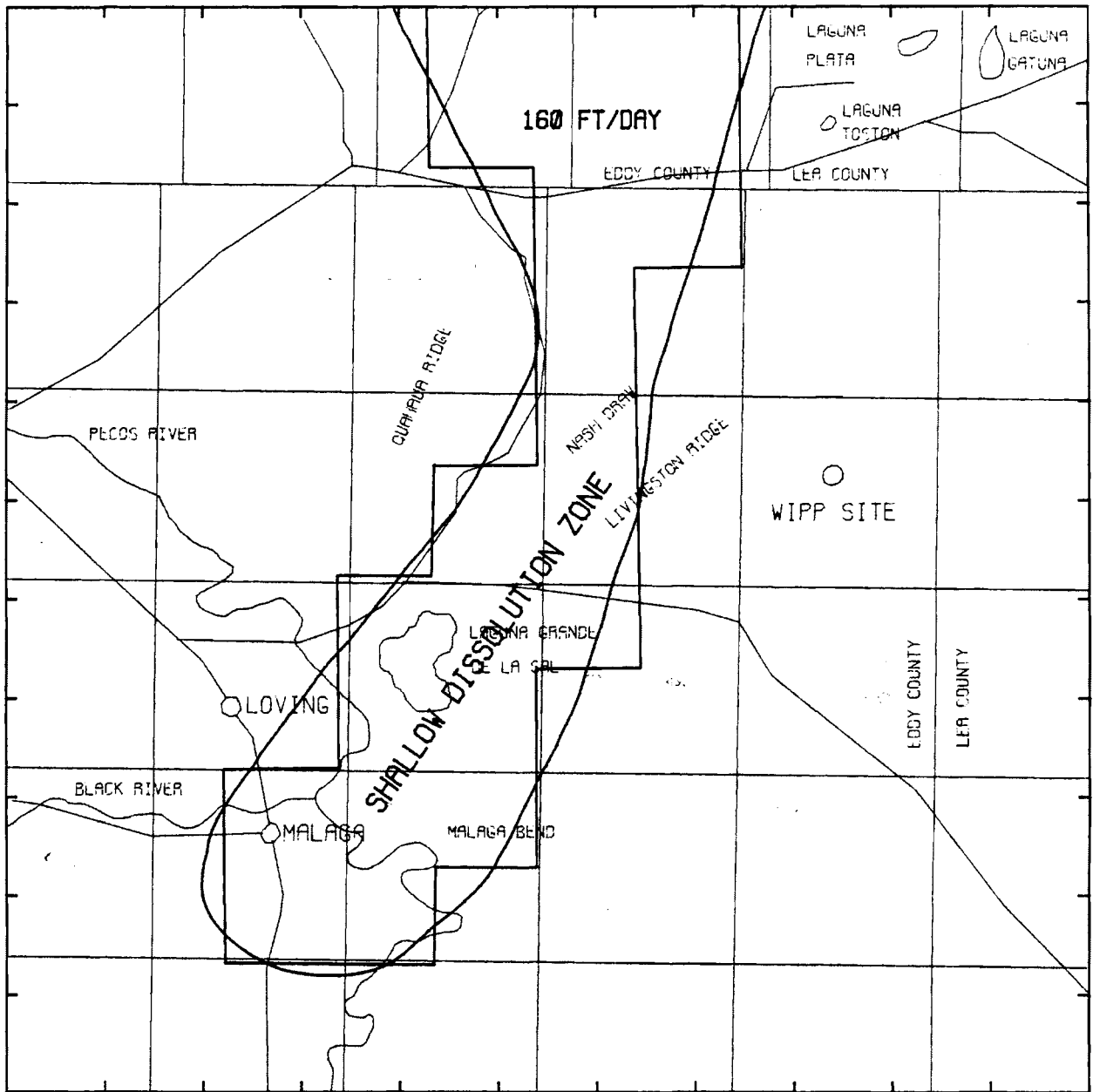


FIGURE 3. Shallow Dissolution Zone Hydraulic Conductivity Distribution (WIPP EIS/ER 1978) Used in the Intera and WISAP Modeling of the WIPP Site

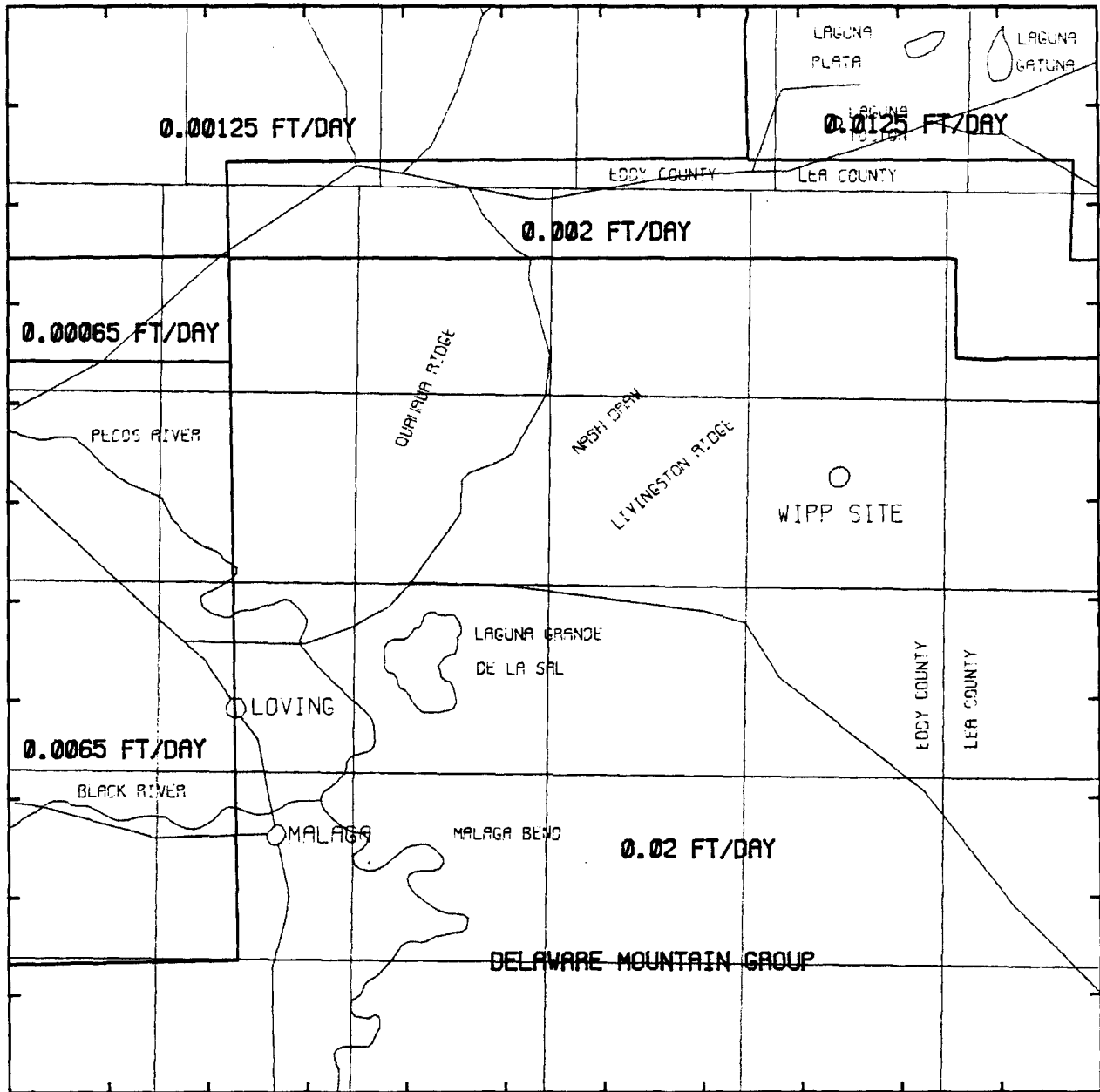


FIGURE 4. Delaware Mountain Group Hydraulic Conductivity Distribution (WIPP EIS/ER 1978) Used in the Intera and WISAP Modeling of the WIPP Site

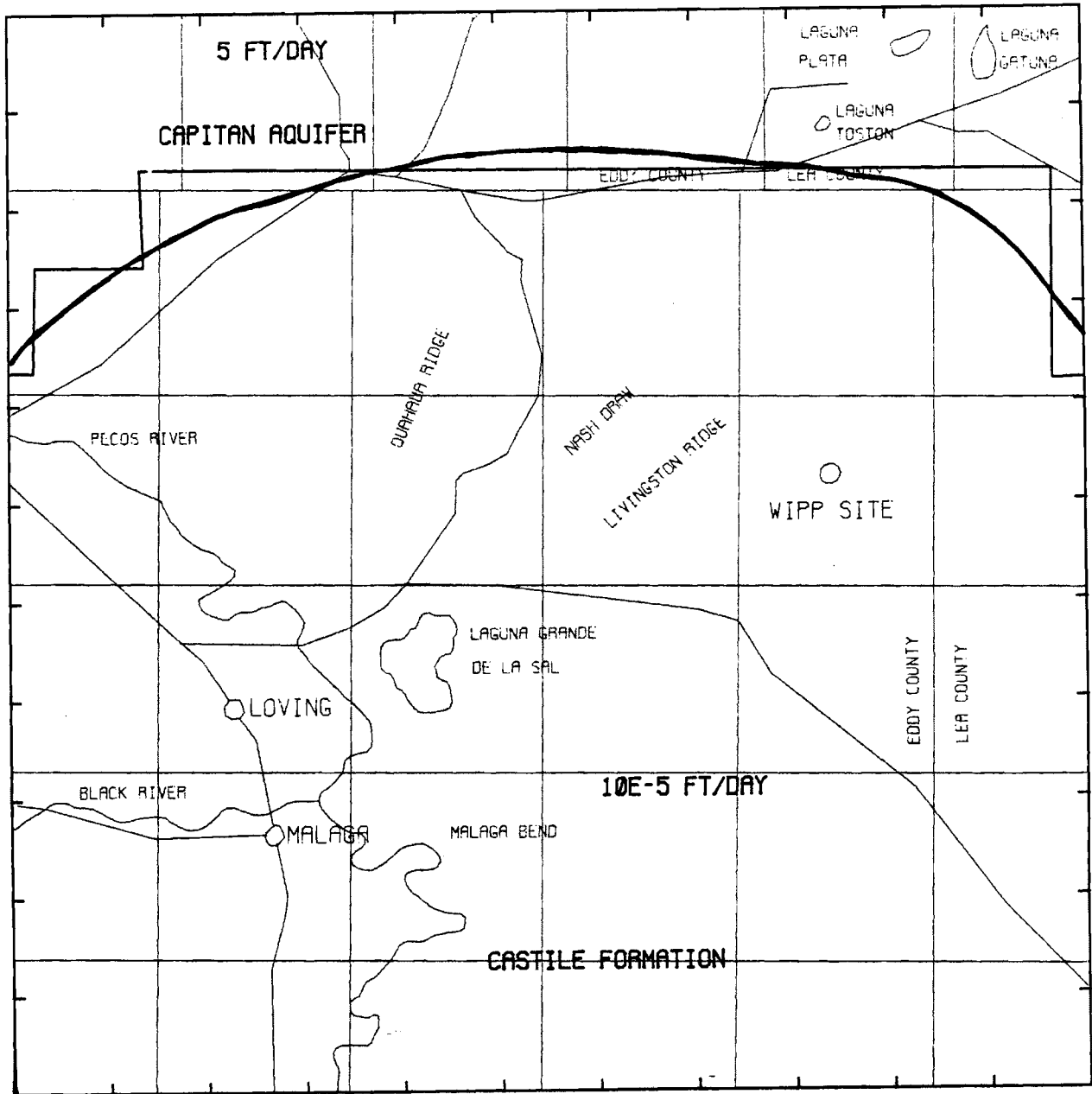
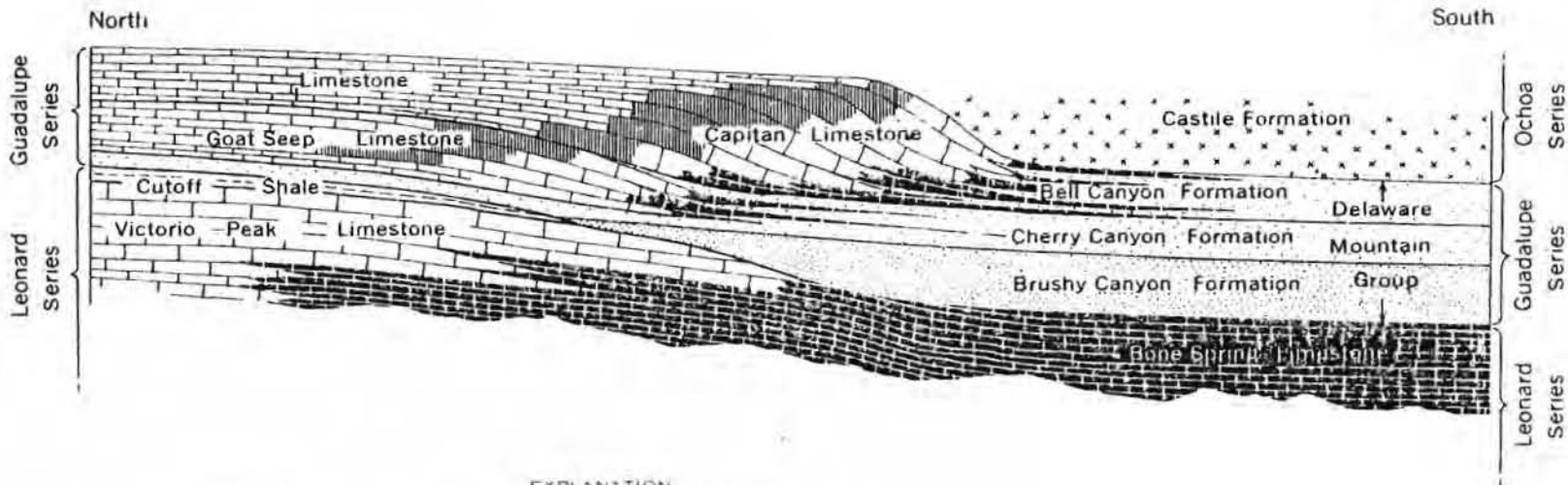
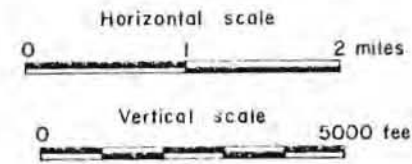
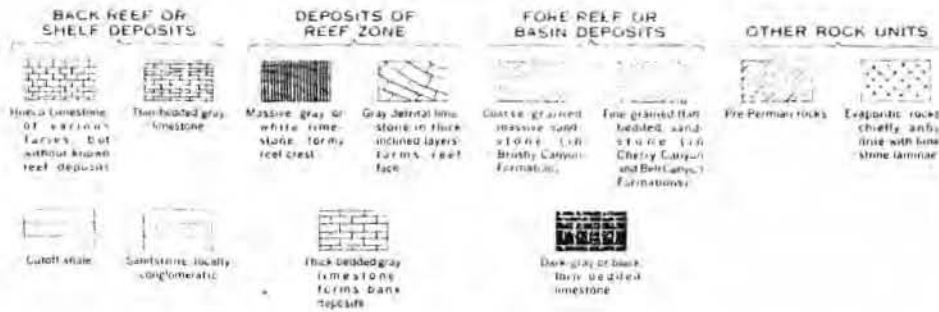


FIGURE 5. Capitan Aquifer Hydraulic Conductivity Distribution (WIPP EIS/ER 1978) Used in the Intera and WISAP Modeling of the WIPP Site



EXPLANATION



Stratigraphic summary of the Guadalupe, Leonard, and adjacent series of the Permian System in the Southern Guadalupe Mountains. The Delaware basin area is to the right and the shelf or platform area is to the left. Rock facies are greatly generalized.

REFERENCE:

- Adapted from E. D. McKee, et al. (1967).
- (Originally compiled from P. B. King (1942, 1948)).

FIGURE 6. Cross Section of Capitan Reef Area (Powers et al. 1979)

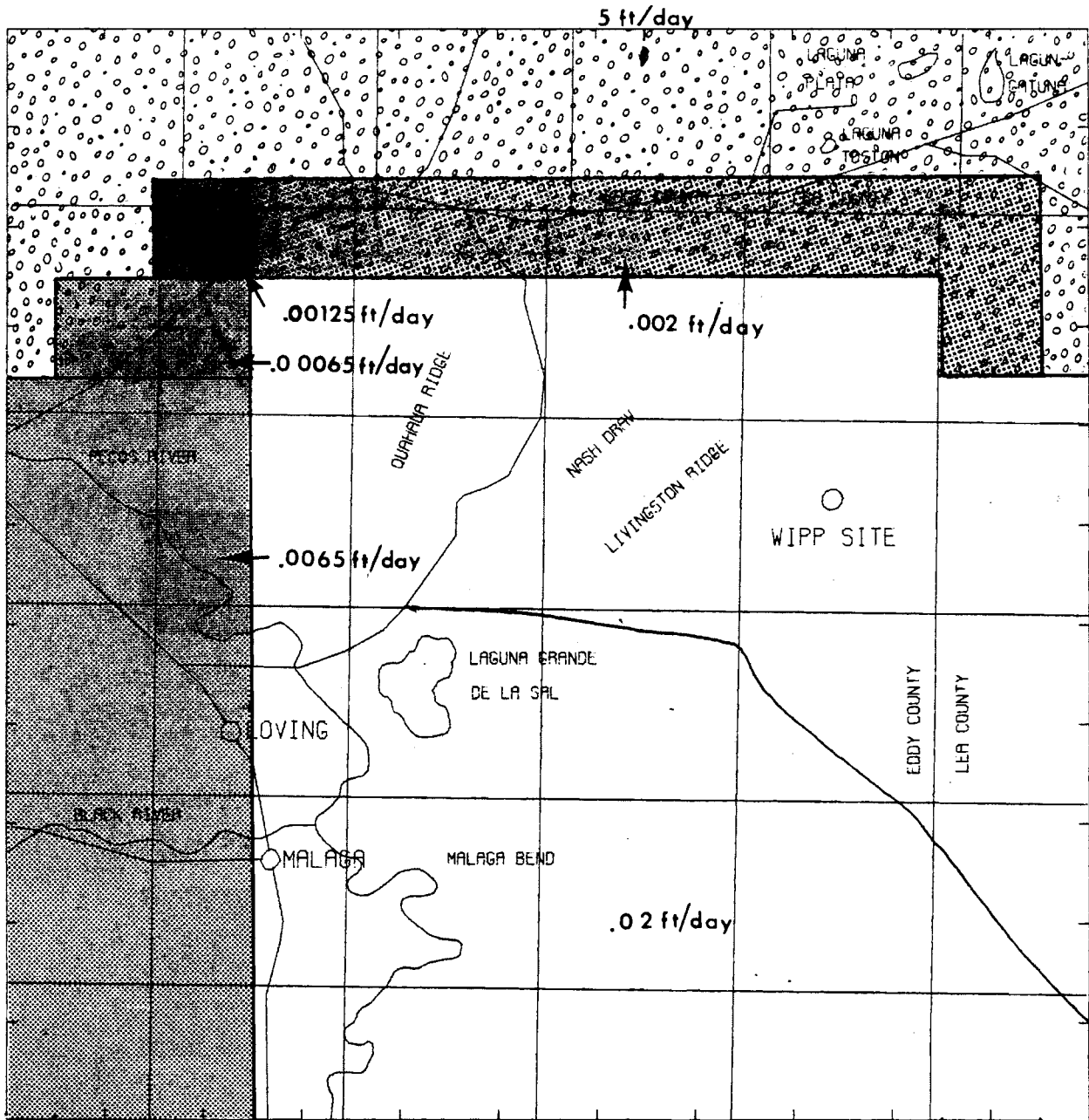


FIGURE 7. WISAP Hydraulic Conductivity Distribution Used to Model the Delaware Mountain-Capitan Aquifer Group

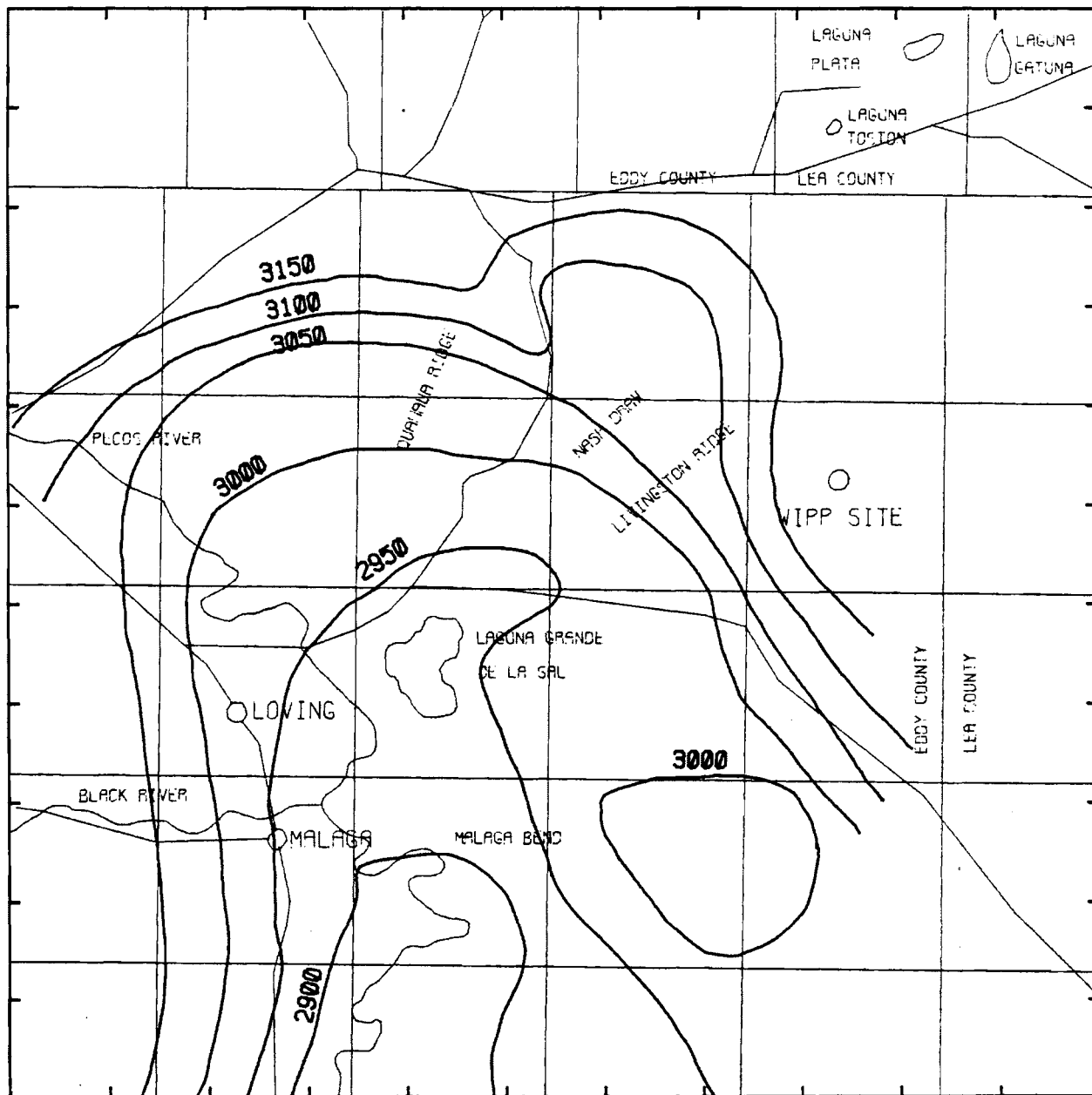


FIGURE 8. Rustler Formation Interpreted or Measured Hydraulic Potentials (WIPP EIS/ER 1978). Contours are in feet referenced to mean sea level.

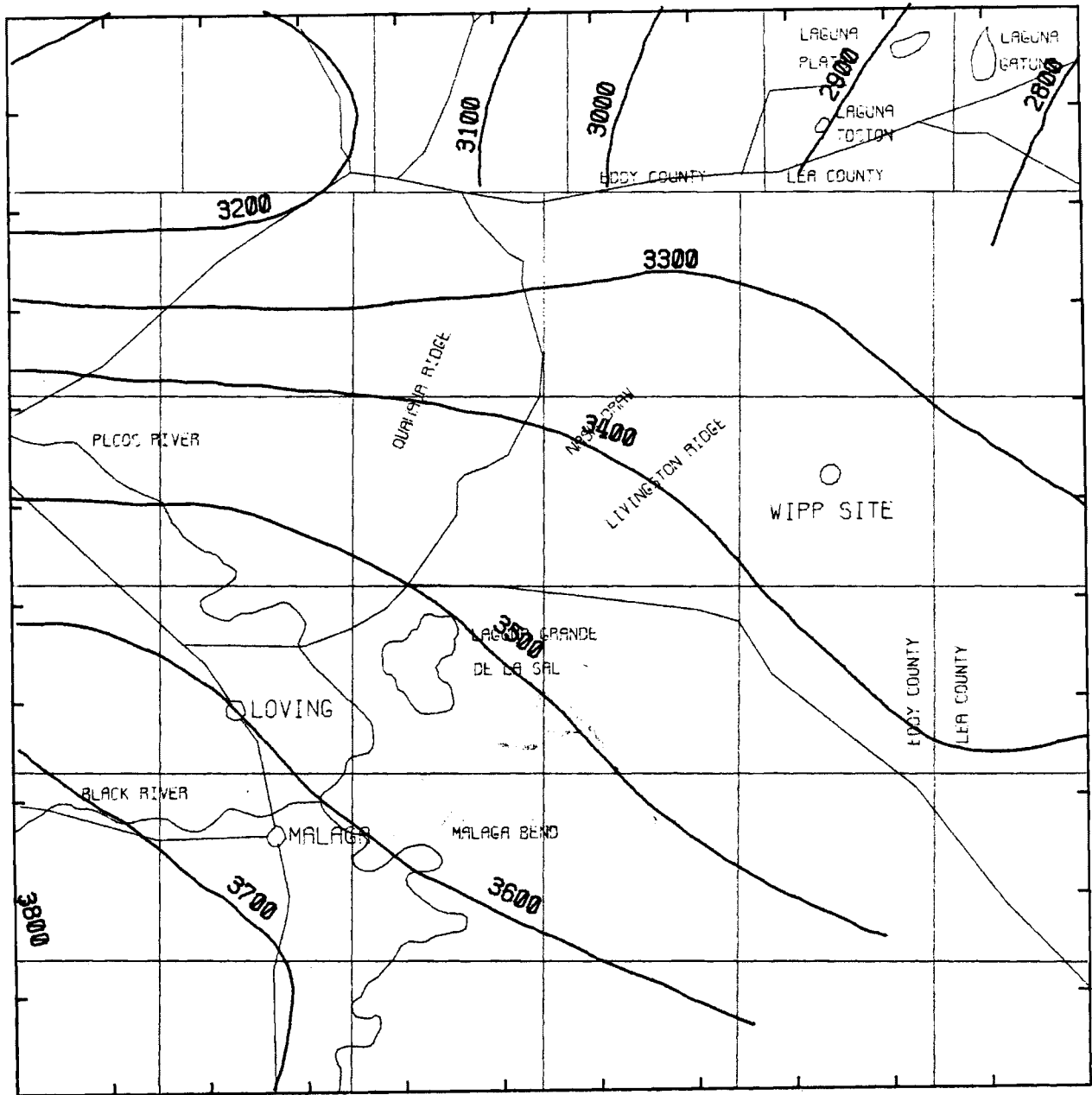


FIGURE 9. Delaware Mountain Group and Capitan Interpreted or Measured Hydraulic Potentials (WIPP EIS/ER 1978). Contours are in feet referenced to mean sea level.

compared to these measured potentials. Intera's model-predicted results for the Rustler and Delaware Mountain Group are shown in Figures 10 and 11, respectively.

WISAP HYDROLOGIC MODEL RESULTS

The WISAP two dimensional multiaquifer Variable Thickness Transient (VTT) model was used to model the Rustler and Delaware Mountain Group Capitan system. The hydraulic conductivity distributions shown in Figures 2 and 7 were used in this WISAP modeling effort. The thickness of the Rustler, Capitan and Delaware Mountain are 40 ft, 1600 ft, and 3000 ft, respectively (WIPP EIS/ER 1978). Porosity was fixed at 0.1 (WIPP EIS/ER 1978). A twelve by twelve grid with a 1.5 mile spacing was used to model each of the two systems as was done in the Intera analysis. Only Dirichlet (held potential) boundary conditions, supplied by Intera for the Rustler, were used in the WISAP analysis. These boundary conditions are indicated by the crossed boxes (nodes) in Figures 12 and 13 for the Rustler and Delaware Mountain-Capitan respectively. Figures 12 and 13 also display the WISAP VTT model-predicted potentials for the Rustler and Delaware Mountain-Capitan aquifer systems. In addition, Figure 12 shows the streamlines from the WIPP site to the discharge site along the Pecos River. The model predicted travel times for these streamlines are shown in Table 1. For the Rustler Formation, the WISAP predicted travel time from the WIPP site to the discharge site is 3600 years. Note that the streamlines shown in Figure 12 converge as they go from regions of low transmissivity to high transmissivity. Table 2 shows the transmissivity distribution used in this WISAP modeling effort. Table 3 shows a node by node comparison between WISAP model predicted potentials and the measured potentials for the two different aquifers. Since the held potential boundary conditions for the Rustler were not taken from Figure 8, the differences shown in Table 2 along the Rustler boundary are not zero.

CONCLUSIONS ON WISAP AND INTERA HYDROLOGIC MODELING COMPARISON

The WISAP hydrologic modeling methodology includes various levels of modeling capability from simple one- and two-dimensional analytical methods

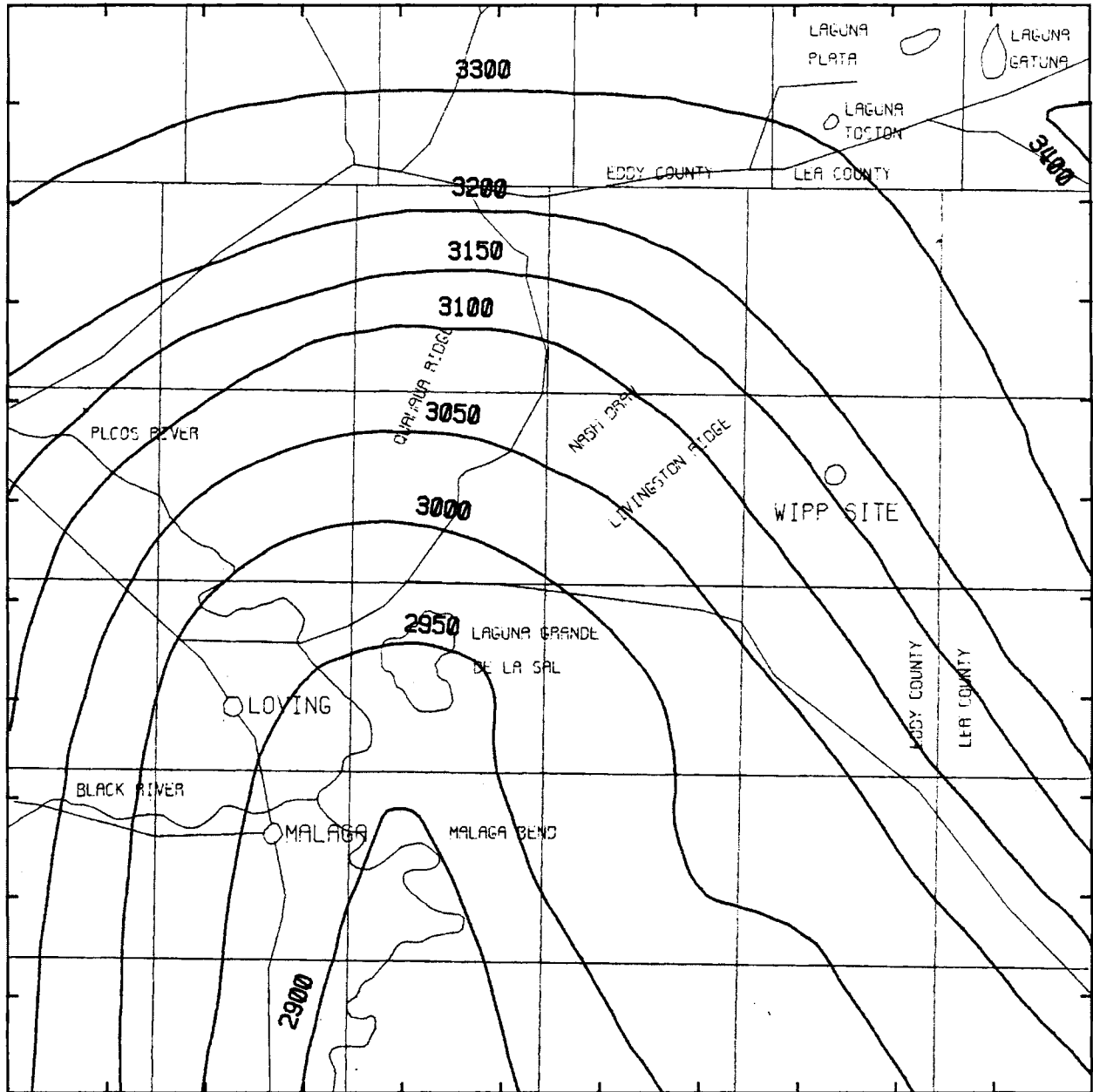


FIGURE 10. Rustler Formation Hydraulic Potentials (WIPP EIS/ER 1978) Calculated by the Intera Model. Contours are in feet referenced to mean sea level.

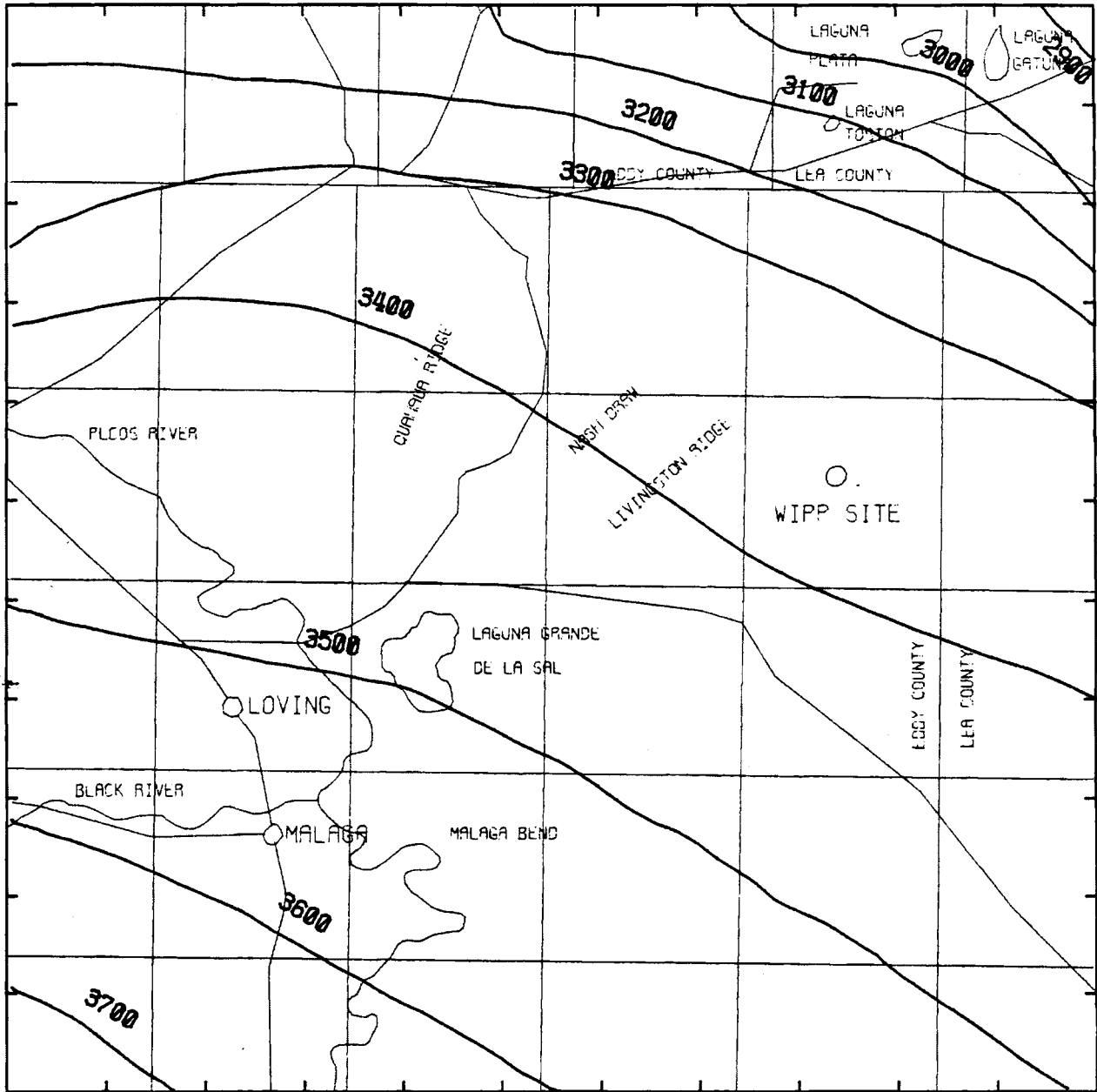


FIGURE 11. Delaware Mountain Group and Capitan Hydraulic Potentials (WIPP EIS/ER 1978) Calculated by the Intera Model. Contours are in feet referenced to mean sea level.

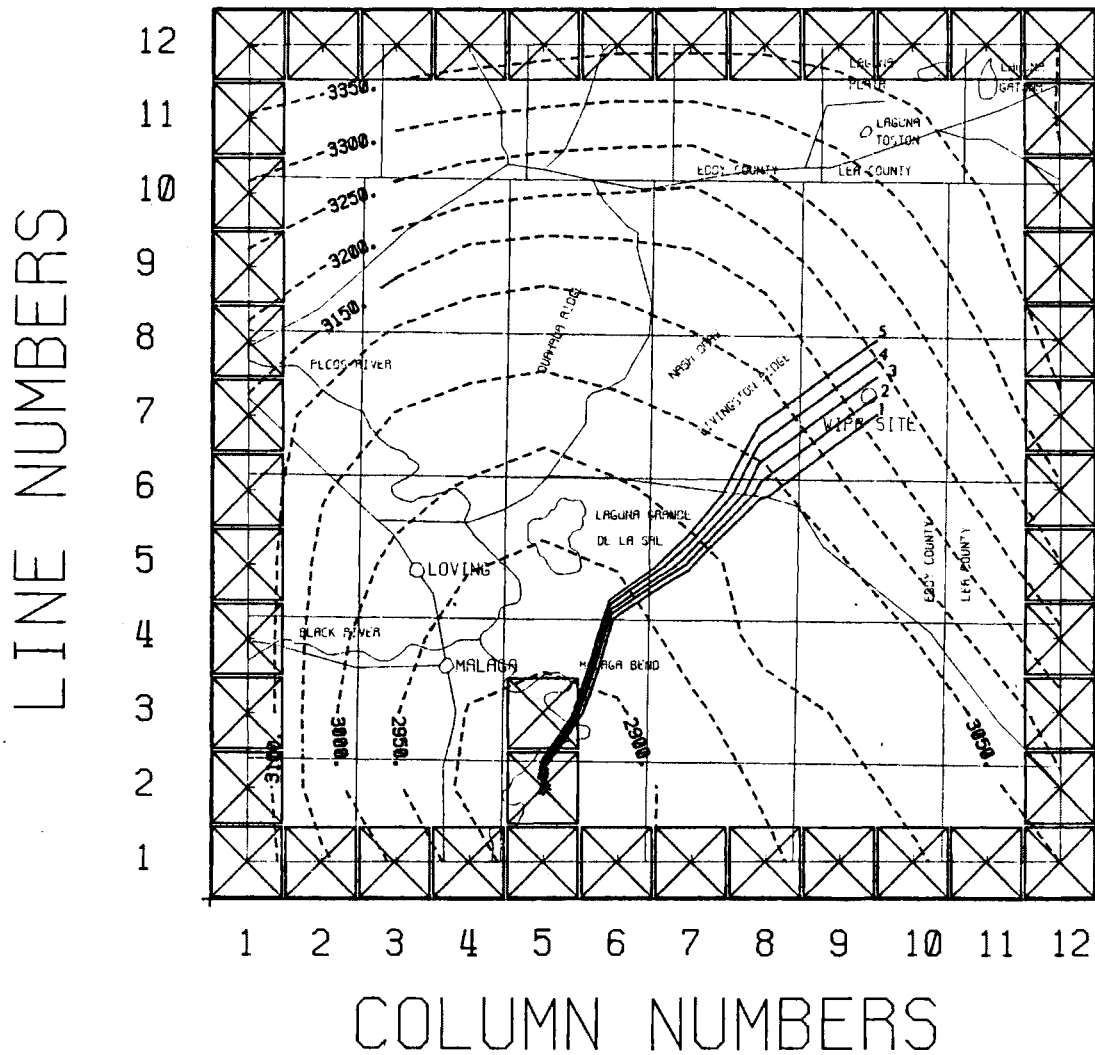


FIGURE 12. Diagram of the Nodal System WISAP Used to Model the Rustler Aquifer. The crossed nodes represent Dirichlet boundary nodes. WISAP model predicted potential distribution is illustrated by the heavy dashed lines and travel paths from the WIPP site are illustrated by the heavy solid lines. Contours are in feet referenced to mean sea level.

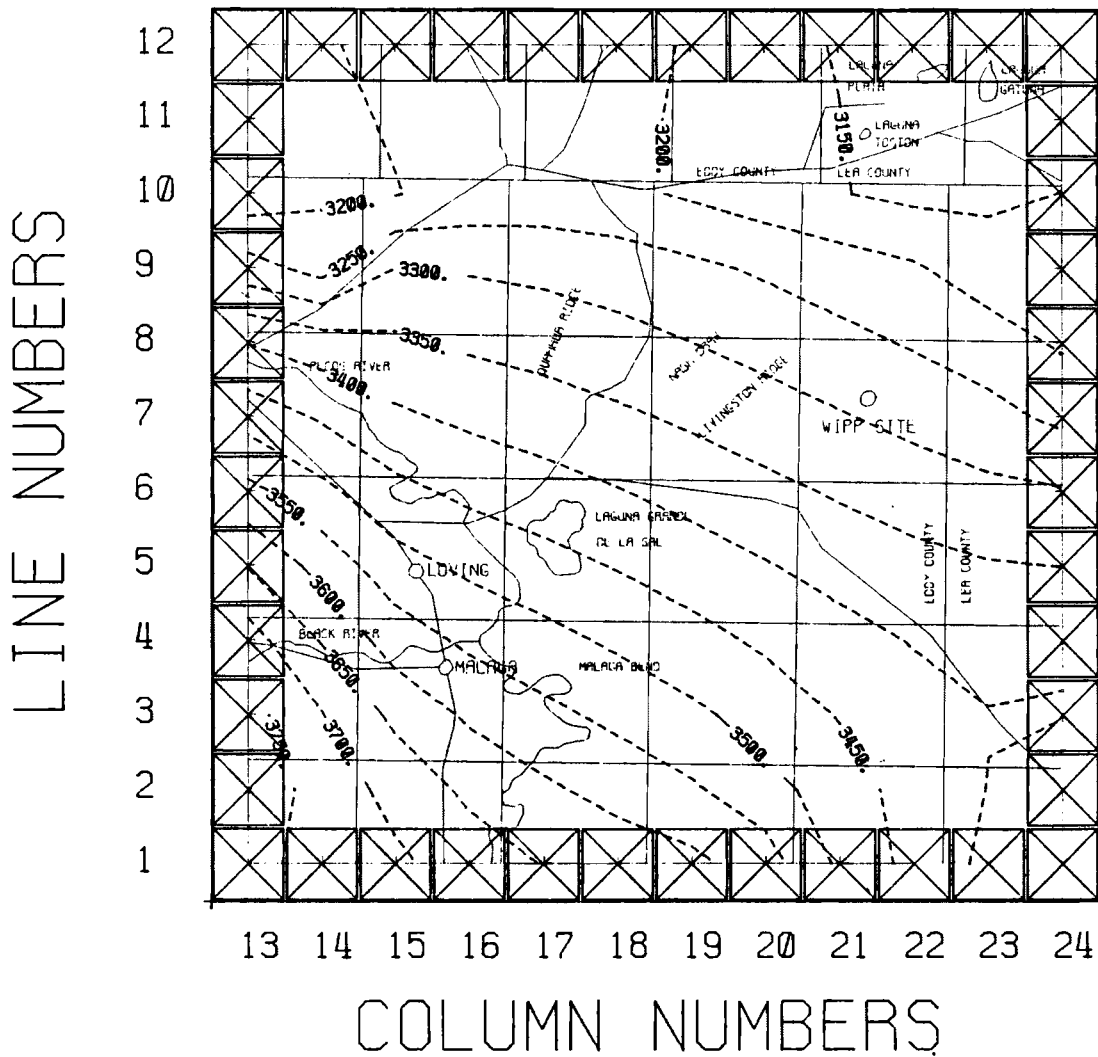


FIGURE 13. Diagram of the Nodal System WISAP Used to Model the Delaware Mountain-Capitan Aquifer System. The crossed nodes represent Dirchlet boundary nodes. WISAP model predicted potential distribution is illustrated by the heavy dashed lines. Contours are in feet referenced to mean sea level.

TABLE 1. WISAP VTT Model Predicted Travel Time for the Five Streamlines Shown in Figure 12

Streamline Data

Aquifer 1

Porosity = 0.1000
 Endpoints of Starting Boundary
 In Node Coordinates

X1 = 9.5000 Y1 = 7.0000
 X2 = 9.5000 Y2 = 8.0000

<u>No.</u>	<u>X-END</u> <u>(node)</u>	<u>Y-END</u> <u>(node)</u>	<u>Time</u> <u>(years)</u>	<u>Distance</u> <u>(feet)</u>
1	4.9438	1.9239	3434.95	114048.0
2	4.9500	1.9654	3572.41	116424.0
3	5.0743	1.9259	3668.15	121176.0
4	5.0888	1.9721	3720.74	123552.0
5	4.9939	1.9056	3824.73	128304.0

Average Time (years) = 3644.20
 Average Distance (feet) = 120701.
 Average Velocity (feet/year) = 33.1214

All starting (X1, Y1, X2, Y2) and ending (X-END, Y-END) coordinates for streamlines are referenced to the line (Y's) and column (X's) coordinate system shown in Figure 12.

through complex three dimensional models, with heat and solute transport. The conceptual model of the WIPP site hydrogeology required the use of the intermediate level VTT model, which is a two-dimensional multilayer finite difference model which solves the Boussinesq equations for ground-water flow and allows the various layers to be connected via an interaquifer transfer coefficient.

Figure 14 shows the comparison between the WISAP VTT hydrologic model results for the Rustler aquifer potential (dashed lines) and the interpreted or measured potentials (solid lines). Figure 15 shows a similar comparison of the WISAP model results for the Delaware Mountain-Capitan aquifer. Figures 16 and 17 show the same kinds of comparisons, but for the Intera model-predicted

TABLE 2. WISAP Transmissivity Distribution Used to Model the Rustler and Delaware Mountain-Capitan Aquifer Systems

RUSTLER													
TRANSMISSIVITY													
	1	2	3	4	5	6	FT**2/DAY	7	8	9	10	11	12
12	40.	40.	40.	40.	40.	40.	40.	40.	40.	40.	40.	40.	40.
11	40.	40.	40.	40.	40.	40.	40.	40.	40.	40.	40.	40.	40.
10	40.	40.	40.	40.	40.	40.	40.	40.	40.	40.	40.	40.	40.
9	40.	40.	40.	40.	40.	40.	160.	40.	40.	40.	40.	40.	40.
8	40.	40.	40.	160.	160.	160.	160.	40.	40.	40.	40.	40.	40.
7	40.	40.	160.	160.	160.	160.	160.	40.	40.	40.	40.	40.	40.
6	40.	40.	160.	160.	160.	160.	160.	40.	40.	40.	40.	40.	40.
5	40.	40.	160.	160.	1280.	160.	160.	160.	160.	40.	40.	40.	40.
4	40.	40.	160.	160.	1280.	160.	160.	160.	160.	160.	40.	40.	40.
3	40.	40.	160.	160.	1280.	160.	160.	160.	160.	160.	160.	40.	40.
2	40.	40.	160.	160.	1280.	160.	160.	160.	160.	160.	160.	160.	40.
1	40.	40.	160.	160.	2560.	160.	160.	160.	160.	160.	160.	160.	160.

DELAWARE MOUNTAIN-CAPITAN

TRANSMISSIVITY													
	13	14	15	16	17	18	FT**2/DAY	19	20	21	22	23	24
12	8000.	8000.	8000.	8000.	8000.	8000.	8000.	8000.	8000.	8000.	8000.	8000.	8000.
11	8000.	8000.	8000.	8000.	8000.	8000.	8000.	8000.	8000.	8000.	8000.	8000.	8000.
10	8000.	8000.	4.	6.	6.	6.	6.	6.	6.	6.	6.	6.	8000.
9	8000.	2.	2.	60.	60.	60.	60.	60.	60.	60.	60.	60.	8000.
8	20.	20.	20.	60.	60.	60.	60.	60.	60.	60.	60.	60.	60.
7	20.	20.	20.	60.	60.	60.	60.	60.	60.	60.	60.	60.	60.
6	20.	20.	20.	60.	60.	60.	60.	60.	60.	60.	60.	60.	60.
5	20.	20.	20.	60.	60.	60.	60.	60.	60.	60.	60.	60.	60.
4	20.	20.	20.	60.	60.	60.	60.	60.	60.	60.	60.	60.	60.
3	20.	20.	20.	60.	60.	60.	60.	60.	60.	60.	60.	60.	60.
2	60.	60.	60.	60.	60.	60.	60.	60.	60.	60.	60.	60.	60.
1	60.	60.	60.	60.	60.	60.	60.	60.	60.	60.	60.	60.	60.

TABLE 3. Node by Node Comparison Between WISAP VTT Model Predicted Potential Distributions in the 2 Aquifers (Figures 12 and 13) and the Measured or Interpreted Potentiometric Distribution (Figures 8 and 9). The maximum and minimum differences as well as the root mean square (R.M.S.) deviations are illustrated. All differences are in feet.

		Rustler Max.=44.8 Min.=-116.5 R.M.S.=37.0											
COLUMN		1	2	3	4	5	6	7	8	9	10	11	12
LINE													
12*	12	24	37	31	35	35	34	25	17	5	-13	-19	
11*	-4	3	0	-7	-4	3	8	15	11	6	-3	-4	
10*	-19	-19	-31	-49	-49	-18	-17	-6	-7	-8	-9	-3	
9*	-34	-31	-39	-62	-77	6	16	-14	-39	-30	-19	0	
8*	-21	2	15	27	10	-12	11	-27	-72	-56	-35	-8	
7*	-6	20	34	39	32	33	-3	-79	-101	-85	-53	-4	
6*	17	1	32	32	21	44	24	-76	-116	-108	-66	-17	
5*	17	-24	9	14	0	-15	4	-19	-84	-89	-81	-28	
4*	6	-47	-17	-1	-9	-47	-36	0	-33	-72	-58	-40	
3*	1	-61	-39	-14	-15	-52	-63	-30	7	-36	-62	-31	
2*	6	-52	-31	-9	-29	-45	-37	-26	1	1	-40	-33	
1*	16	3	32	45	-22	-28	-26	-24	-1	1	-24	-45	

		Delaware Mountain-Capitan Max.=45.4 Min.=-75.8 R.M.S.=27.5											
COLUMN		1	2	3	4	5	6	7	8	9	10	11	12
LINE													
12*	0	0	0	0	0	0	0	0	0	0	0	0	
11*	0	21	20	17	-5	-6	5	-2	-14	-19	-13	0	
10*	0	20	12	18	-10	-14	-3	-24	-40	-44	-28	0	
9*	0	-30	45	39	21	5	-12	-24	-22	-13	-18	0	
8*	0	-15	-20	-26	-28	-33	-43	-48	-43	-18	-2	0	
7*	0	-37	-64	-60	-54	-53	-51	-44	-34	-23	-3	0	
6*	0	-44	-76	-70	-57	-52	-45	-34	-22	-11	-5	0	
5*	0	-42	-70	-64	-51	-42	-34	-23	-9	1	-5	0	
4*	0	-28	-56	-48	-39	-32	-22	-14	-6	-3	-15	0	
3*	0	-14	-43	-40	-30	-26	-19	-15	-21	-20	-20	0	
2*	0	-13	-32	-28	-22	-24	-30	-34	-40	-25	-13	0	
1*	0	0	0	0	0	0	0	0	0	0	0	0	

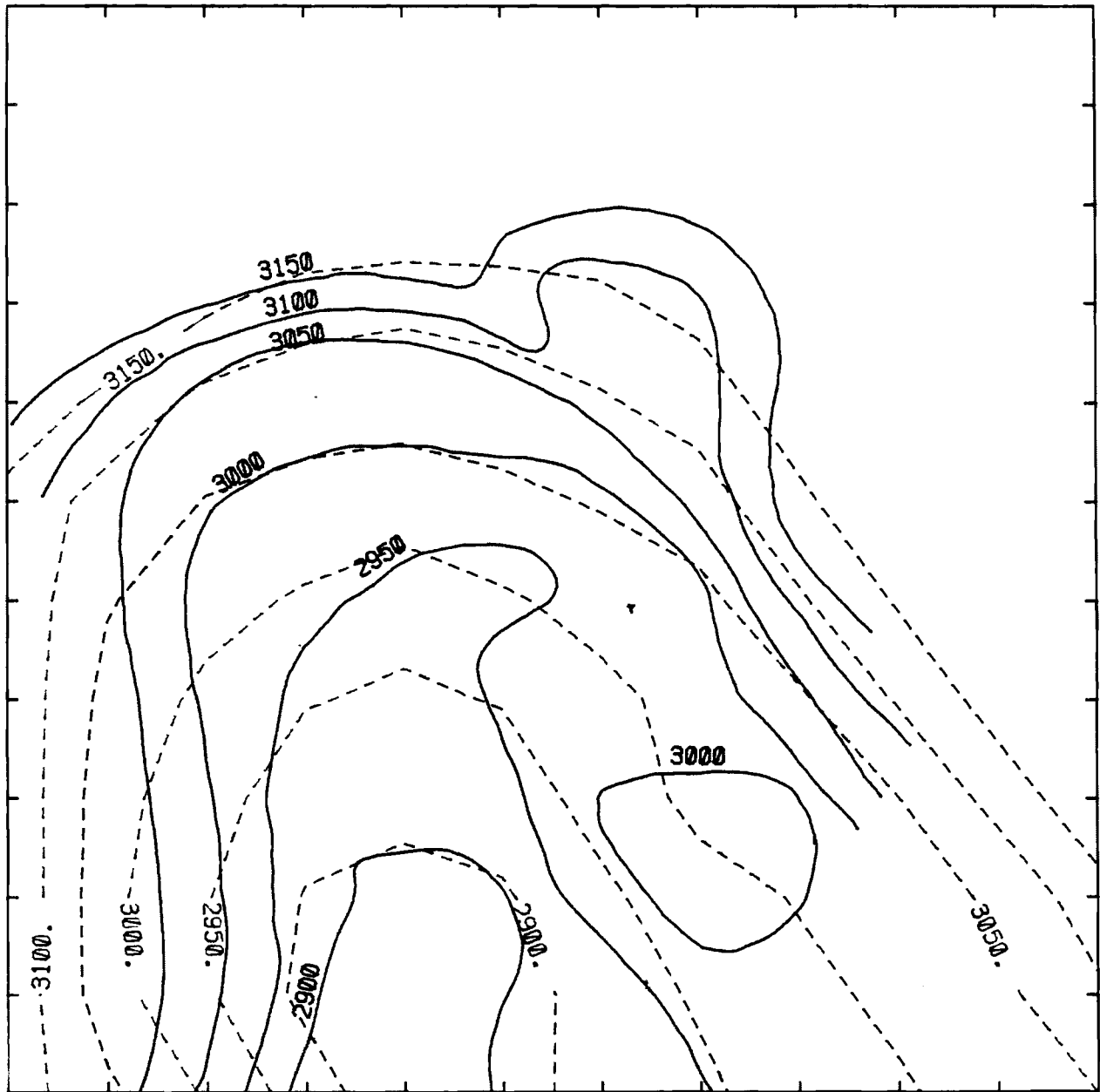


FIGURE 14. Plot Showing the Comparison Between the WISAP VTT Model Predicted Potentials for the Rustler (dashed lines) and the Measured or Interpreted Potentials (WIPP EIS/ER 1978) (solid lines). All contours are in feet referenced to mean sea level.

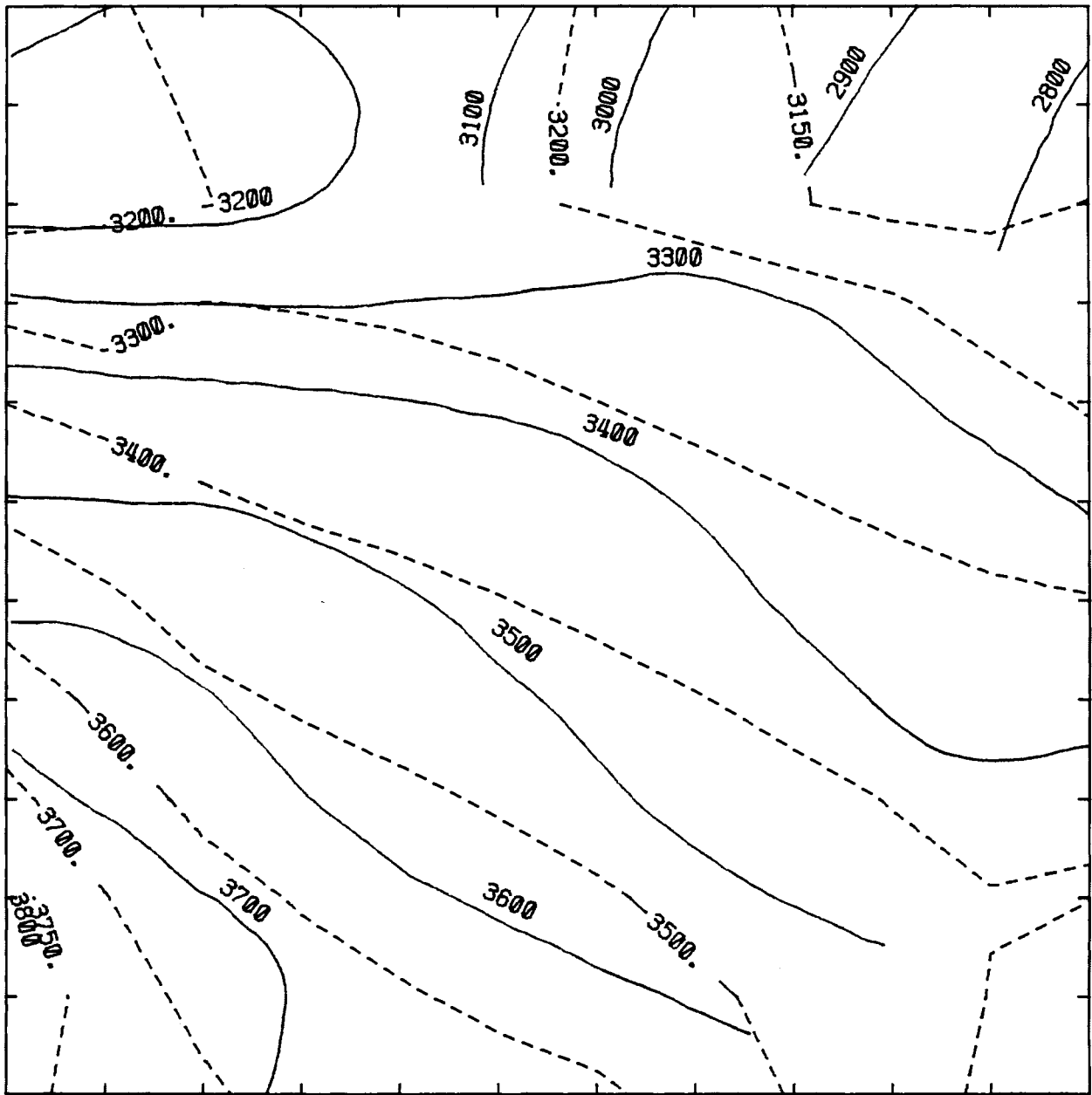


FIGURE 15. Plot Showing the Comparison Between the WISAP VTT Model Predicted Potentials for the Delaware Mountain-Capitan (dashed lines) and the Measured or Interpreted Potentials (WIPP EIS/ER 1978) (solid lines). All contours are in feet referenced to mean sea level.

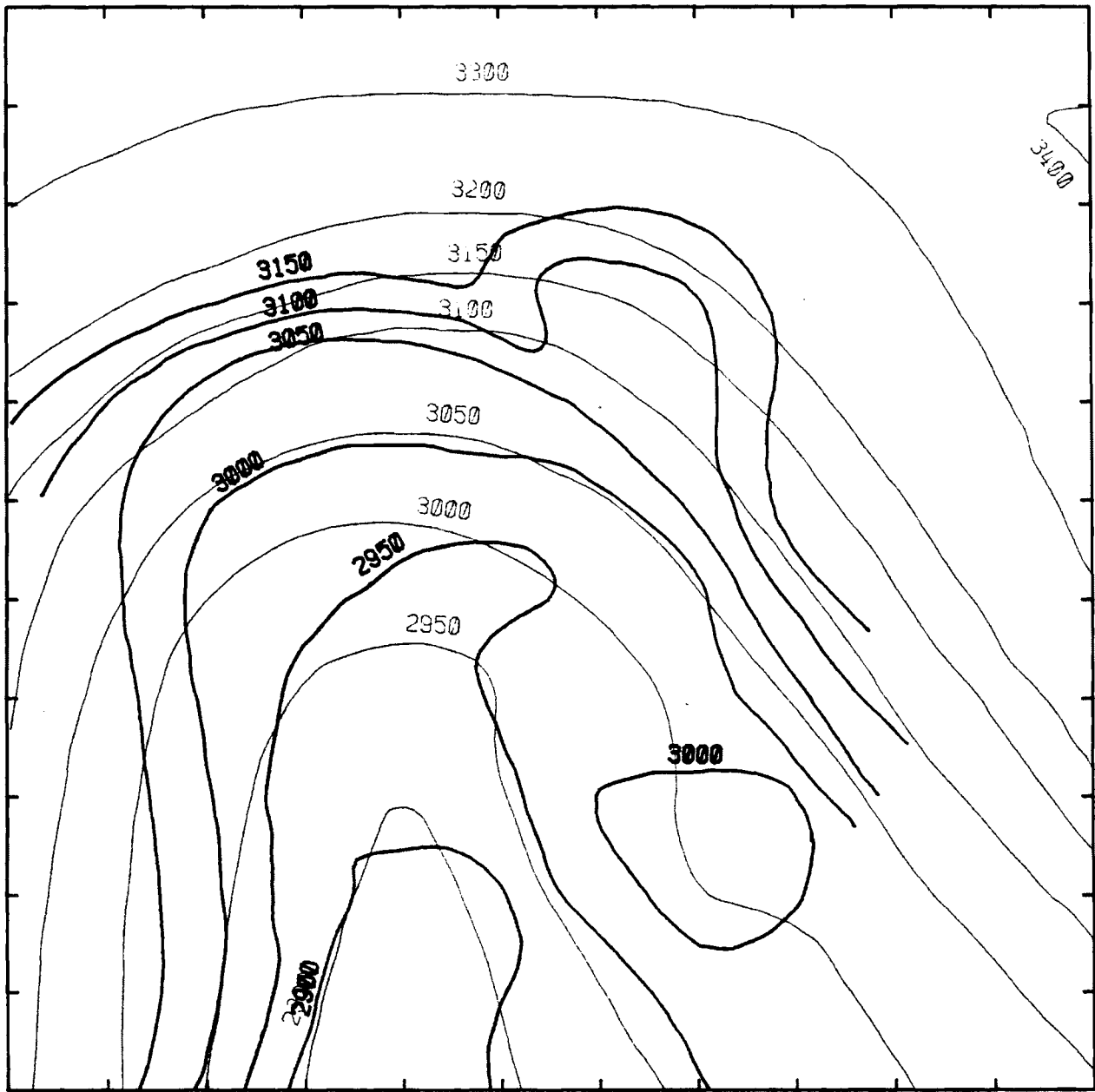


FIGURE 16. Plot Showing the Comparison Between the WIPP Intra Model Predicted Potentials (WIPP EIS/ER 1978) for the Rustler (light lines) and the Measured or Interpreted Potentials (WIPP EIS/ER 1978) (heavy lines). All contours are in feet referenced to mean sea level.

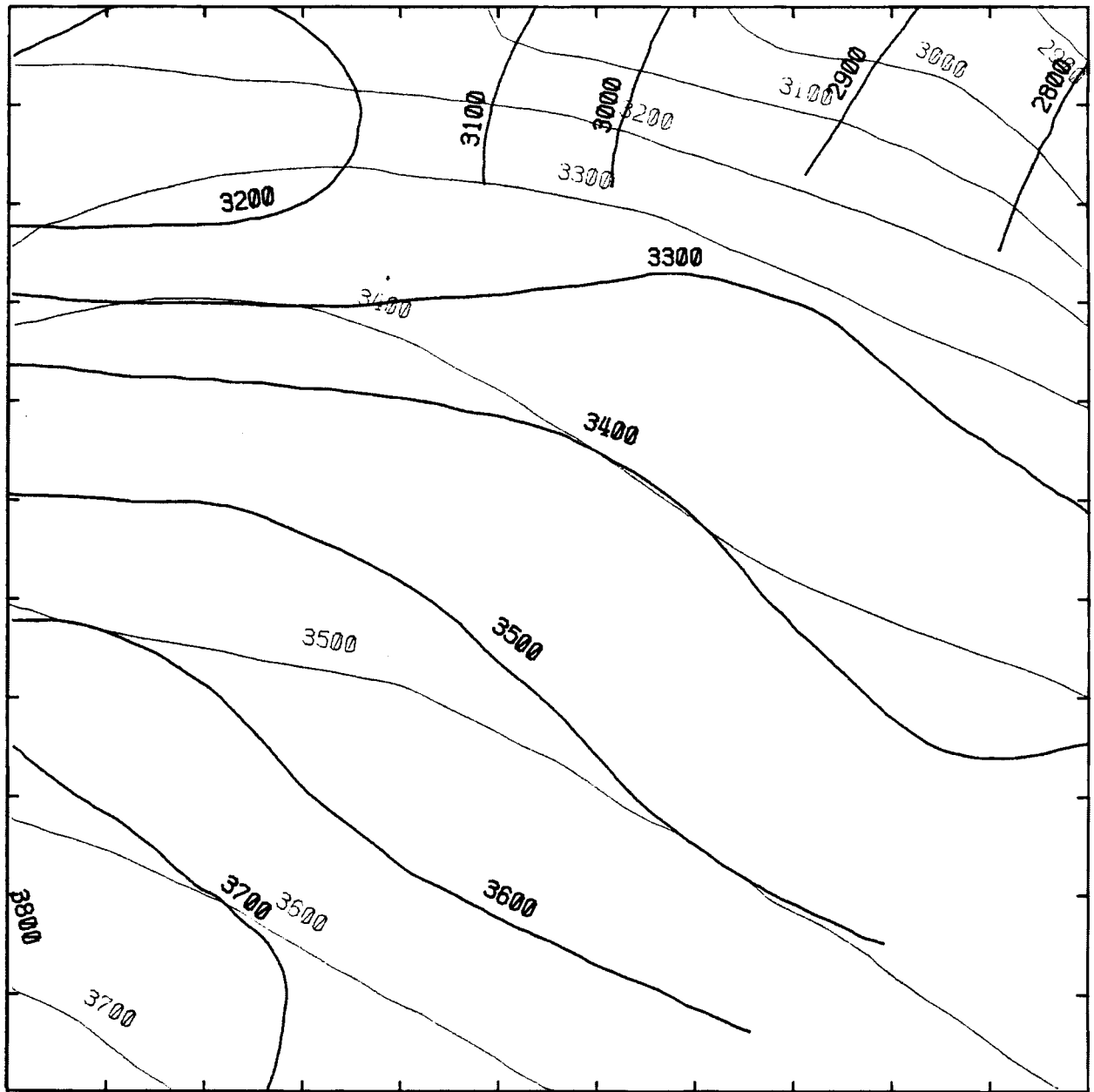


FIGURE 17. Plot Showing the Comparison Between the Intra Model Predicted Potentials (WIPP EIS/ER 1978) for the Delaware Mountain-Capitan (light lines) and the Measured or Interpreted Potentials (WIPP EIS/ER 1978) (heavy lines). All contours are in feet referenced to mean sea level.

potentials for the Rustler and Delaware Mountain-Capitan, respectively. Heavy solid lines represent the interpreted data and light solid lines represent the Intera model results. A comparison between the WISAP VTT model results (dashed lines) and the Intera model results (solid lines) for the Rustler and Delaware Mountain-Capitan are shown in Figures 18 and 19, respectively. The slight differences between the WISAP VTT model results and the Intera model results for the Rustler can be most likely attributed to the slightly different methods used for the boundary conditions. Dirichlet (held potential) boundaries were used for the WISAP VTT model at each of the crossed nodes in Figures 12 and 13, whereas the Intera model used aquifer influence functions along the boundary. Differences between WISAP VTT model results and Intera model results for this Delaware Mountain-Capitan are due to the somewhat different conceptual model explained earlier.

In order to make a comparison between the WISAP and Intera travel times, the Intera potential distribution shown in Figure 10 was digitized on a 12 by 12 grid and the streamline and travel times were calculated for this potential distribution and the hydraulic conductivity distribution shown in Figure 2. Figure 20 shows the contours of the digitized Intera potential distribution and five predicted streamlines originating at the WIPP area. Table 4 shows the node by node comparison between the measured or interpreted potentials (Figures 8 and 9) and the digitized Intera model predicted potentials. Table 5 lists the travel times and path lengths for the 5 streamlines shown in Figure 20.

The Rustler potential comparison between WISAP and Intera agree fairly well. The Delaware Mountain-Capitan are different but this was because of the different conceptual interpretation used for this aquifer system. Table 6 shows a comparison between the WISAP VTT and Intera travel time results. Travel times for the Rustler streamlines agree very well. The average distances and velocities show some deviation, but this can be explained by noting that the VTT streamlines terminate farther downstream and thus travel an additional 27,000 ft in the higher hydraulic conductivity zone. Since the velocity is averaged along the path length this results in the greater average velocity.

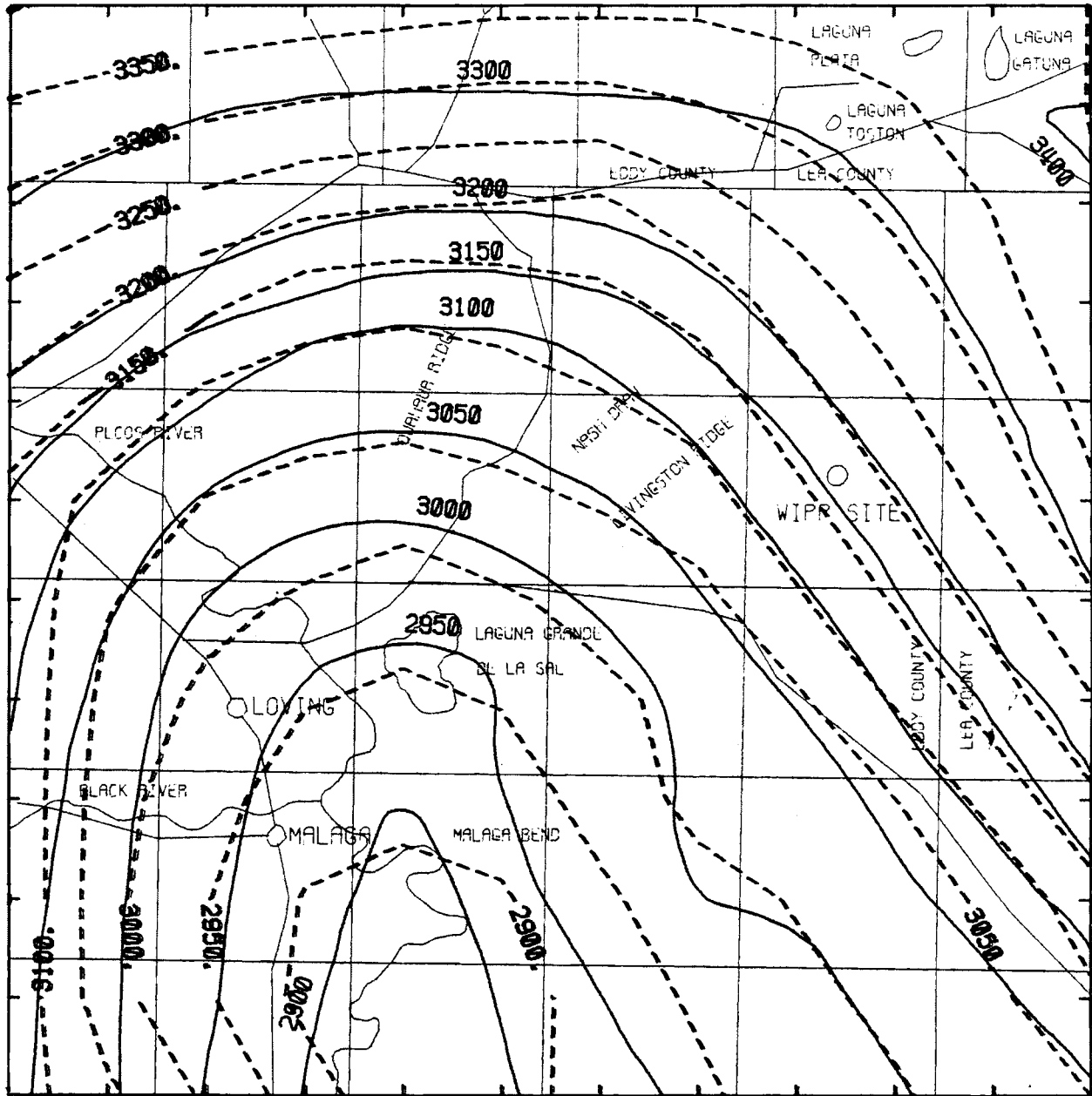


FIGURE 18. Plot Showing the Comparison Between the WISAP VTT Model Predicted Potentials for the Rustler (dashed lines) and the Intra Model Predicted Potentials (WIPP EIS/ER 1978) (solid lines). All contours are in feet referenced to mean sea level.

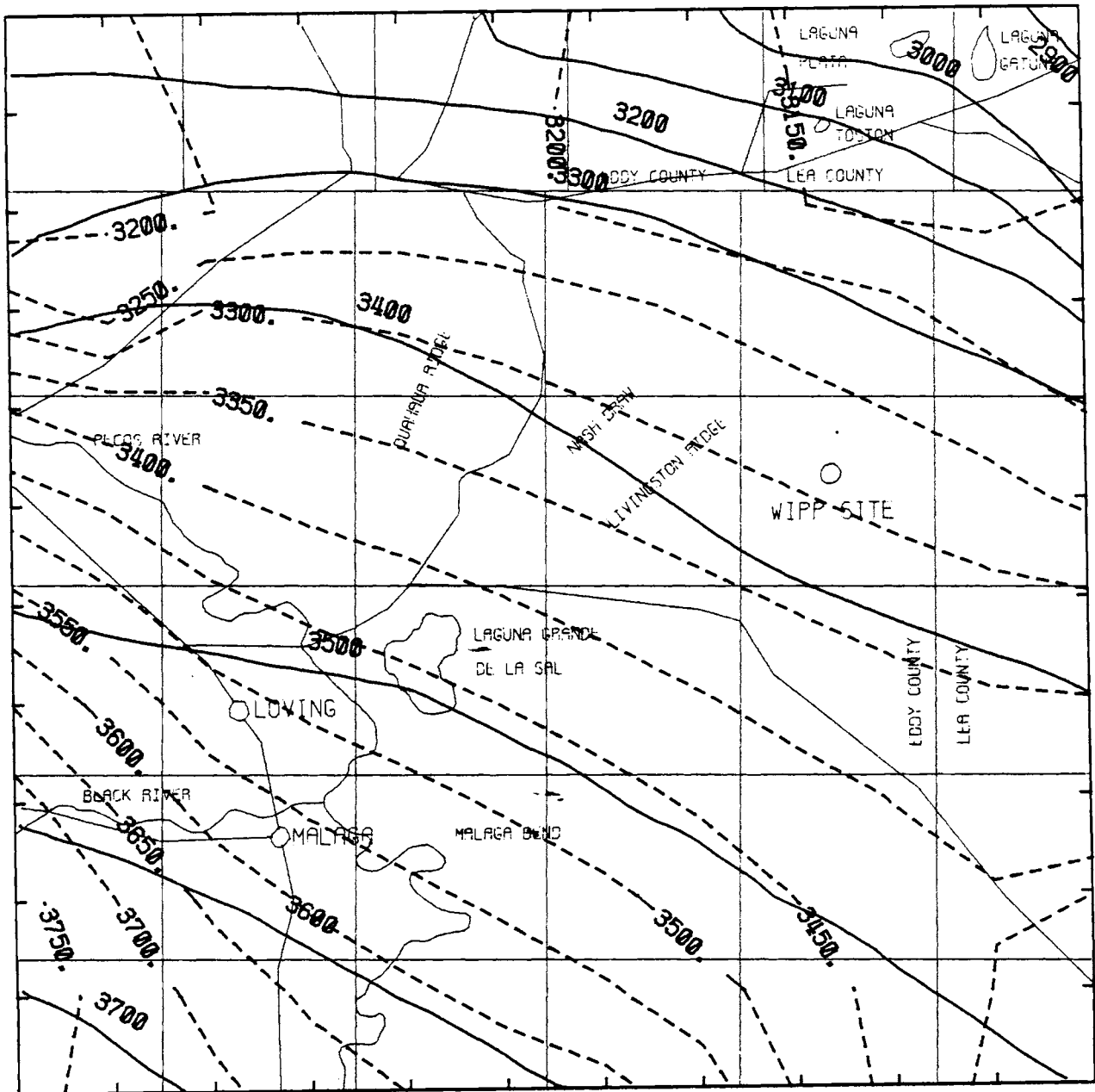


FIGURE 19. Plot Showing the Comparison Between the WISAP VTT Model Predicted Potentials for the Delaware Mountain-Capitan (dashed lines) and the Intera Model Predicted Potentials (WIPP EIS/ER 1978) (solid lines). All contours are in feet referenced to mean sea level.

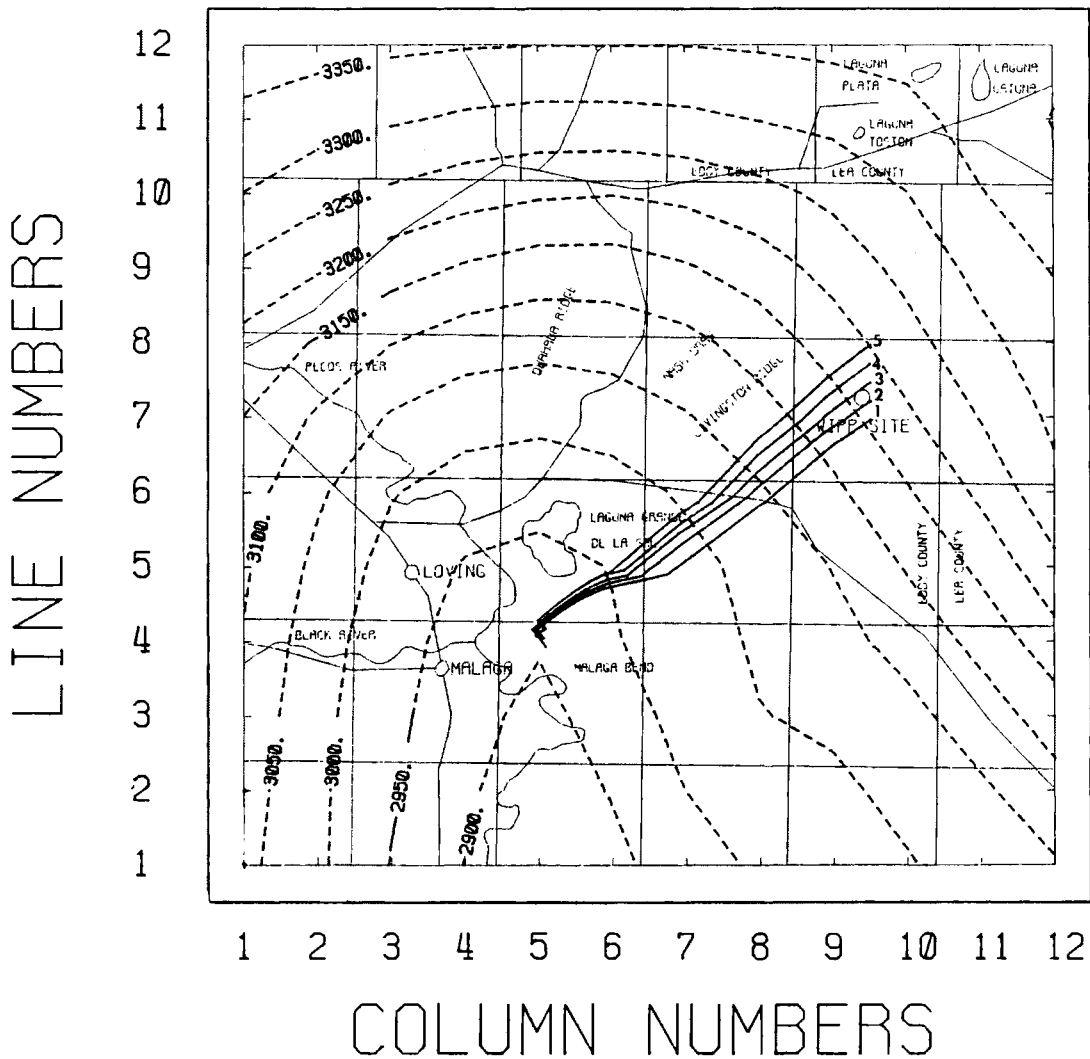


FIGURE 20. Intera Predicted Potentials and the Associated Streamlines from the WIPP Site. All contours are in feet referenced to mean sea level.

The results of the WISAP modeling of the WIPP hydrologic system indicate that for the same conceptual model (i.e., hydrologic interpretation), essentially the same results are achieved as those obtained with the Intera model. This result was expected since the various hydrologic codes essentially utilize and solve the same flow equations.

TABLE 4. Node by Node Comparison Between the Intera Model Predicted Potential Distributions (WIPP EIS/ER 1978) in the 2 Aquifers (Figures 10 and 11) and the Measured or Interpreted Potential Distributions (WIPP EIS/ER 1978) (Figures 8 and 9). The maximum difference and minimum difference as well as the root mean square (R.M.S.) deviations are illustrated. All differences are in feet.

Rustler Max.=31.0 Min.=-119.2 R.M.S.=37.5

COLUMN	*****											
	1	2	3	4	5	6	7	8	9	10	11	12
LINE												
12*	-10	-2	5	9	18	26	26	22	12	-1	-21	-34
11*	-13	-4	-6	-13	-7	6	14	18	4	-6	-2	-3
10*	-12	-17	-29	-44	-45	-16	3	-5	-17	-20	-14	-14
9*	-31	-26	-28	-39	-63	11	24	-6	-45	-41	-34	-38
8*	-23	9	31	29	14	-17	3	-26	-78	-63	-50	-47
7*	7	30	31	24	18	19	-15	-77	-110	-92	-66	-36
6*	-1	5	18	16	23	30	16	-67	-119	-119	-77	-25
5*	-19	-21	1	6	-9	-15	0	-19	-74	-89	-92	-38
4*	-46	-46	-14	4	-20	-26	-26	-7	-22	-55	-60	-49
3*	-66	-60	-30	8	-11	-21	-36	-11	13	-25	-46	-38
2*	-62	-62	-33	13	-21	-16	-7	-9	4	4	-36	-42
1*	-49	-49	-13	17	-44	-28	-9	-6	0	4	-25	-48

Delaware Mountain-Capitan Max.=145.5 Min.=-226.5 R.M.S.=76.0

COLUMN	*****											
	1	2	3	4	5	6	7	8	9	10	11	12
LINE												
12*	-11	-17	-35	-54	-81	-130	-126	-142	-161	-160	-186	-227
11*	58	61	49	30	-4	-17	-16	-39	-73	-101	-151	-200
10*	107	129	138	128	93	87	105	70	30	-2	-48	-159
9*	96	132	145	137	112	90	71	59	63	64	48	-7
8*	29	39	51	57	59	54	40	32	37	63	84	107
7*	-19	-22	-15	4	16	20	23	29	38	49	75	94
6*	-68	-67	-53	-27	-5	6	16	27	40	52	58	63
5*	-107	-93	-68	-38	-17	1	16	29	46	57	49	50
4*	-135	-99	-70	-38	-18	-2	14	30	45	52	35	29
3*	-121	-93	-79	-46	-26	-12	4	21	31	34	35	51
2*	-135	-68	-66	-46	-33	-27	-23	-8	16	52	78	101
1*	-1	-22	-18	-17	-16	-18	-20	4	64	100	126	136

TABLE 5. Predicted Travel Times for the Five Streamlines Which Were Derived from the Intera Model Potentiometric Distribution (WIPP EIS/ER 1978) in Figure 20 and the Hydraulic Conductivity Distribution Used in the Intera Model and Shown in Figure 2

Streamline Data

Aquifer 1

Porosity = 0.1000
Endpoints of Starting Boundary
In Node Coordinates

X1 = 9.5000 Y1 = 7.0000
X2 = 9.5000 Y2 = 8.0000

<u>No.</u>	<u>X-END (node)</u>	<u>Y-END (node)</u>	<u>Time (years)</u>	<u>Distance (feet)</u>
1	5.0611	4.0785	3387.31	87912.0
2	5.0204	4.0765	3384.51	90288.0
3	5.0895	3.9701	3448.30	95040.0
4	4.9629	4.1209	3502.28	95040.0
5	4.9939	4.1131	3492.96	97416.0

Average Time (years) = 3443.07
Average Distance (feet) = 93139.
Average Velocity (feet/year) = 27.0512

All starting (X1, Y1, X2, Y2) and ending (X-END, Y-END) coordinates for streamlines are referenced for the line (Y's) and column (X's) coordinate system shown in Figure 20.

TABLE 6. Comparison Between the WISAP and Intera Travel Time Results

	<u>VTT</u>	<u>Intera</u>
Average travel for the five Rustler streamlines from the WIPP area, years	3644.	3443.
Average velocity for the five Rustler streamlines from the WIPP area, feet/year	33.12	27.1
Average travel distance for the five Rustler streamlines from the WIPP area, feet	120701.	93139.

TRANSPORT MODELING

In modeling the transport of nuclides from WIPP to the discharge site, Intera used a one-dimensional transport model. Based on the streamlines analyzed for the two-dimensional model runs, this should give an adequate representation of transport.

Intera's one-dimensional transport model is coupled with the flow model. After Intera ran the two-dimensional flow model to predict water travel times, a one-dimensional flow model was set up to simulate transport of the nuclides. The Intera one-dimensional simulation was set up by modeling the flow path from the WIPP Site to the Pecos River, which had been predicted with their 3-D model. Intera set up the 1-D model, by utilizing the hydraulic conductivity distribution along the 3-D model flow path. The potentials at the ends of the flow path from the three-dimensional model were also preserved. The Intera transport simulation was then run using the hydrologic conditions described in this 1-D flow tube. Table 7 illustrates the characteristics of the one dimensional flow tube use by Intera.

Although Intera ran various scenarios at upper and lower permeability bounds, WISAP comparison runs were made only for the upper permeability bound

TABLE 7. Characteristics of the One-Dimensional Flow Tube Used by Intera to Simulate the Transport From WIPP to Malaga Bend. These same values were used in the WISAP transport modeling.

1-D flow tube velocity	14.78 ft/yr
1-D flow tube length	78,000 ft
1-D flow tube width	750 ft
1-D flow tube height	40 ft
1-D flow tube velocity	0.1
1-D flow tube dispersivity	300 ft
1-D flow tube bulk density	120 lb/ft ³
β = bulk density/porosity	17.3 g/ml
1-D water travel time	5,277 years

and only for transport of wastes from the spent fuel repository and for repository breach or failure scenario 1 (WIPP EIS/ER 1978). This breach scenario, developed at Sandia, involves flow through the repository as a result of interconnection of the Rustler and Delaware Mountain aquifers through an uncased bore hole centered in the spent fuel repository. The Sandia-Intera analysis indicated a slight head differential between these two aquifer systems, which resulted in a calculated bore hole flow of 600 ft³/day (WIPP EIS/ER 1978). Waters entering the bore hole from the Delaware Mountain aquifer at 230,000 ppm salt (WIPP EIS/ER 1978) were assumed to pick up salt uniformly along the 2,700 ft (WIPP EIS/ER 1978) of uncased salt and exit to the Rustler aquifer at 410,000 ppm salt (WIPP EIS/ER 1978). The 600 ft³/day of water flow would thus result in the loss of 54 ft³ (WIPP EIS/ER 1978) of salt per day from the sides of the bore hole over the entire 2,700 ft of bedded salt (2×10^{-2} ft³ of salt/ft of bore hole/day). The waste in the spent fuel repository (which is 16.5 ft thick and 1,076 ft by 1112 ft in area) was assumed to dissolve at the same rate as the salt and thus would take 164,000 yr to leach into Rustler aquifer waters.

Repository failure for scenario 1 was assumed to occur 1,000 yr after repository sealing. Table 8 lists the spent fuel and TRU inventories (WIPP EIS/ER 1978) in the repository after 1000 years, and the Kd and half-life numbers (WIPP EIS/ER 1978) used in the Intera and WISAP transport modeling. The WISAP 1-D MTT model was used to analyze the transport of wastes from the WIPP site to Malaga Bend for comparison to Intera results. The data in Tables 7 and 8, considering the 164,000 yr leach time, represent all the data necessary to run the WISAP transport model.

For this failure scenario only the 3 fission products (⁹⁹Tc, ¹²⁹I, and ¹³⁵Cs) and the four actinide chains shown in Table 8 are of interest for WISAP transport model studies. Only the longer lived members of the four actinide chains are modeled. Shorter lived members are assumed to be in secular equilibrium with their parents.

TABLE 8. WIPP Repository Inventory at 1,000 yr, for the Modeled Nuclides Along With the Half Life and Kd Values Used in the Intera and WISAP Transport Model (WIPP EIS/ER 1978)

ISOTOPE	HALF LIFE (YEARS)	UNCONTROLLED WATER RADIATION STANDARD (M.P.C.)	KD (ML/G)	TRU WASTE (MICRO-CURIES/LITER)*		SPENT FUEL (MICRO-CURIES/LITER)**	
99-Tc	2.13E5	3.0E-4	0.	0.	0.	1.36E-2	6.59E3
129-I	1.59E7	6.0E-4	0.	0.	0.	3.09E-2	1.50E1
135-Cs	2.3 E6	1.0E-4	15.	0.	0.	3.23E-4	1.56E2
244-Pu	8.3 E7	4.0E-6	2100.	0.	0.	7.62E-15	3.69E-9
240-Pu	6.54E3	5.0E-6	2100.	6.13E7	9.28E6	.419	2.03E5
236-U	2.34E7	3.0E-5	10.	1.94E-2	2.79E2	2.89E-4	1.40E2
232-Th	1.4 E10	2.0E-6	2200.	4.50E-10	6.81E-6	1.39E-11	6.68E-6
237-Np	2.14E6	3.0E-6	700.	8.67E-2	1.31E3	9.09E-4	439.74
233-U	1.59E5	3.0E-5	10.	2.2E-4	3.33	2.97E-6	1.44
229-Th	7.3 E3	7.0E-6	2200.	7.23E-6	1.10E-1	1.21E-7	5.86E-2
242-Pu	3.87E5	5.0E-6	2100.	0.	0.	1.37E-3	6.64E2
238-U	4.47E9	4.0E-5	10.	0.	0.	2.96E-4	1.43E2
238-Pu	8.78E1	5.0E-6	2100.	1.03E-1	1.56E3	0.	0.
234-U	2.44E5	3.0E-5	10.	8.51E-2	1.29E3	1.79E-3	8.67E2
230-Th	7.7 E4	2.0E-6	2200.	6.29E-4	9.51	1.43E-5	6.93
226-Ra	1.6 E3	3.0E-4	25.	1.05E-4	1.59	2.59E-6	1.25
243-Am	7.37E3	4.0E-6	1450.	0.	0.	1.72E-2	8.33E3
239-Pu	2.4 E4	5.0E-6	2100.	2.72E3	4.12E7	0.304	1.47E5
235-U	7.04E8	3.0E-5	10.	2.65E-3	4.01E1	1.6E-5	7.75
231-Pa	3.25E4	9.0E-7	10.	0.	0.	0.	0.

* CONVERSION FACTOR TO CONVERT MICRO-CURIES/LITER TO CURIES (1.514E4). TRU WASTES.

** CONVERSION FACTOR TO CONVERT MICRO-CURIES/LITER TO CURIES (4.843E5). SPENT FUEL WASTES.

TRANSPORT MODEL RESULTS

The WISAP one-dimensional MMT transport model was run for the 3 fission products and 4 actinide chains shown in Table 8. The results of the WISAP transport model are shown in Figures 21 through 35 in the form of Malaga Bend arrival curves. These graphs illustrate the concentration versus time of the various nuclides in the groundwater, which is being discharged at Malaga Bend into the Pecos River. Isotopes not displayed have decayed before reaching Malaga Bend. Table 9 summarizes the WISAP MMT transport model results. This table indicates the minimum and maximum times of discharge (years), the total number of curies released to the environment (Ci), the time of peak arrival (years), peak concentration ($\mu\text{Ci}/\text{ml}$) in the groundwater and Pecos River water along with the respective ratios to maximum permissible concentration (MPC) (U.S. ERDA 1975), and the peak release rate (Ci/yr) to the Pecos River. For purposes of these calculations, the Pecos River flow rate was assumed to be 0.736 cubic meters per second (WIPP EIS/ER 1978). Only two isotopes arrived at Malaga Bend with ground-water concentration above the maximum permissible uncontrolled water radiation standard (MPC). These isotopes were 129-I (1.23 times MPC) and 226-Ra (4.83 times MPC). Dilution by the Pecos River brought both of these concentrations in the biosphere river below MPC.

TRANSPORT MODELING CONCLUSIONS

Transport model comparisons will be made when the Intera transport model results are received. Preliminary runs, made earlier in this study with a different leach time and a slightly different flow tube description, indicated that the transport models give comparable results.

KD= 0.00 ML/G HALF-LIFE=2.1300E+05 YEARS BETA= 17.3 G/ML
INITIAL INVENTORY=6.5870E+03 CURIES. PRESENT INVENTORY=5.0173E+03 CURIES.
ISOTOPE TC-99 FLOW TUBE 1 CONCENTRATION VS TIME

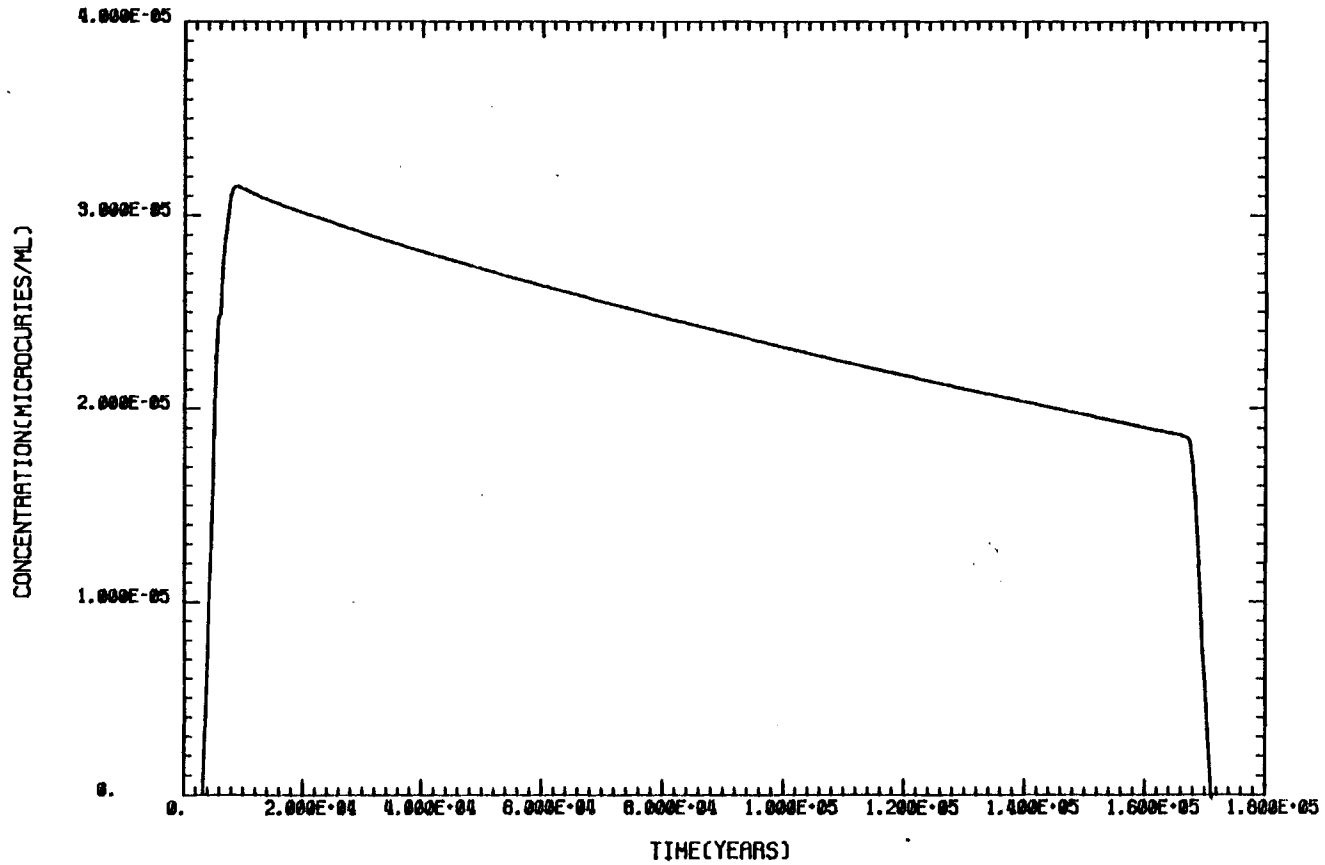


FIGURE 21. WISAP Predicted Malaga Bend Arrival Curve for Tc-99

KD= 0.00 ML/G HALF-LIFE=1.5900E+07 YEARS BETA= 17.3 G/ML
INITIAL INVENTORY=1.4970E+01 CURIES. PRESENT INVENTORY=1.4913E+01 CURIES.
ISOTOPE I-129 FLOW TUBE 1 CONCENTRATION VS TIME

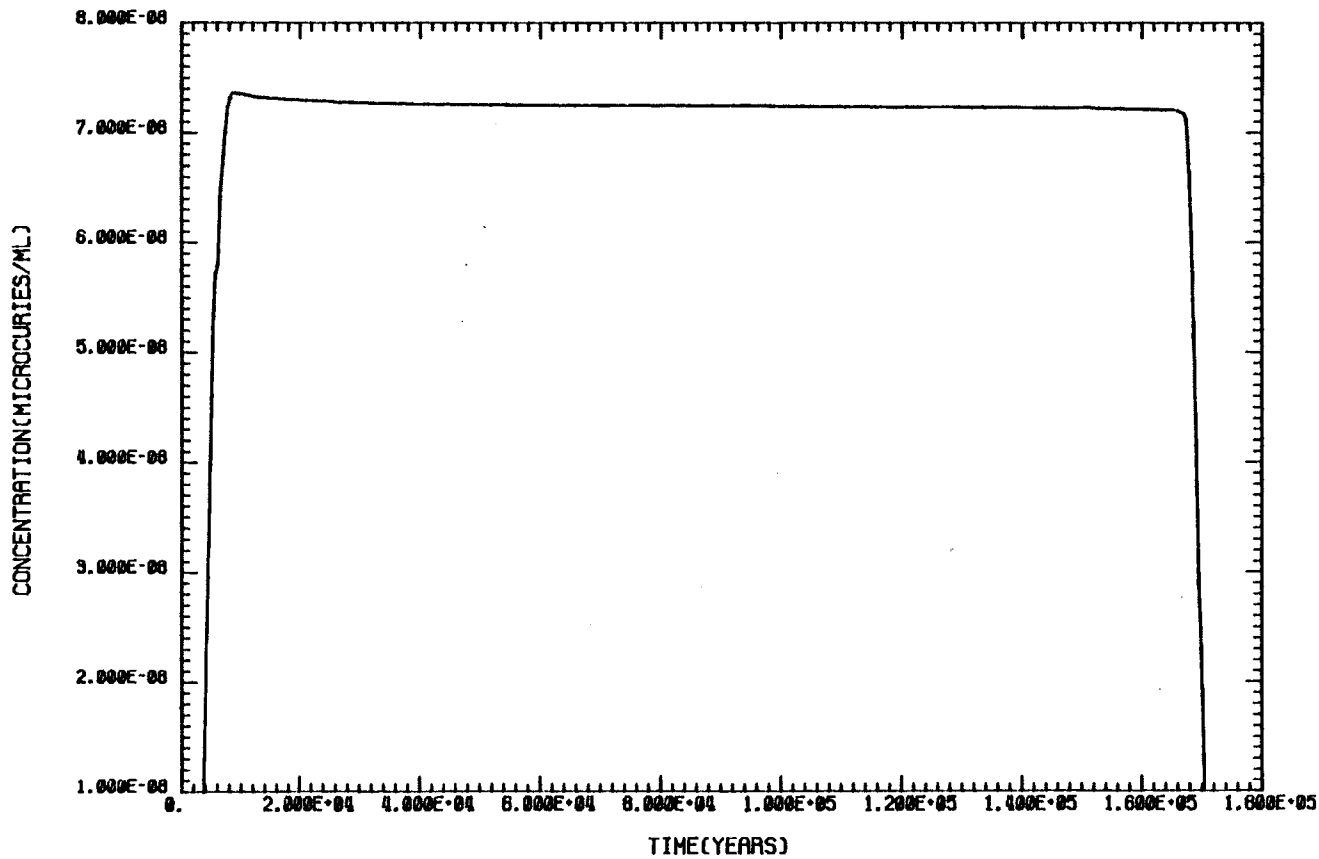


FIGURE 22. WISAP Predicted Malaga Bend Arrival Curve For I-129

KD= 15.00 ML/G HALF-LIFE=2.3000E+06 YEARS BETA= 17.3 G/ML
INITIAL INVENTORY=1.5640E+02 CURIES. PRESENT INVENTORY=1.0000E+02 CURIES.
ISOTOPE CS-135 FLOW TUBE 1 CONCENTRATION VS TIME

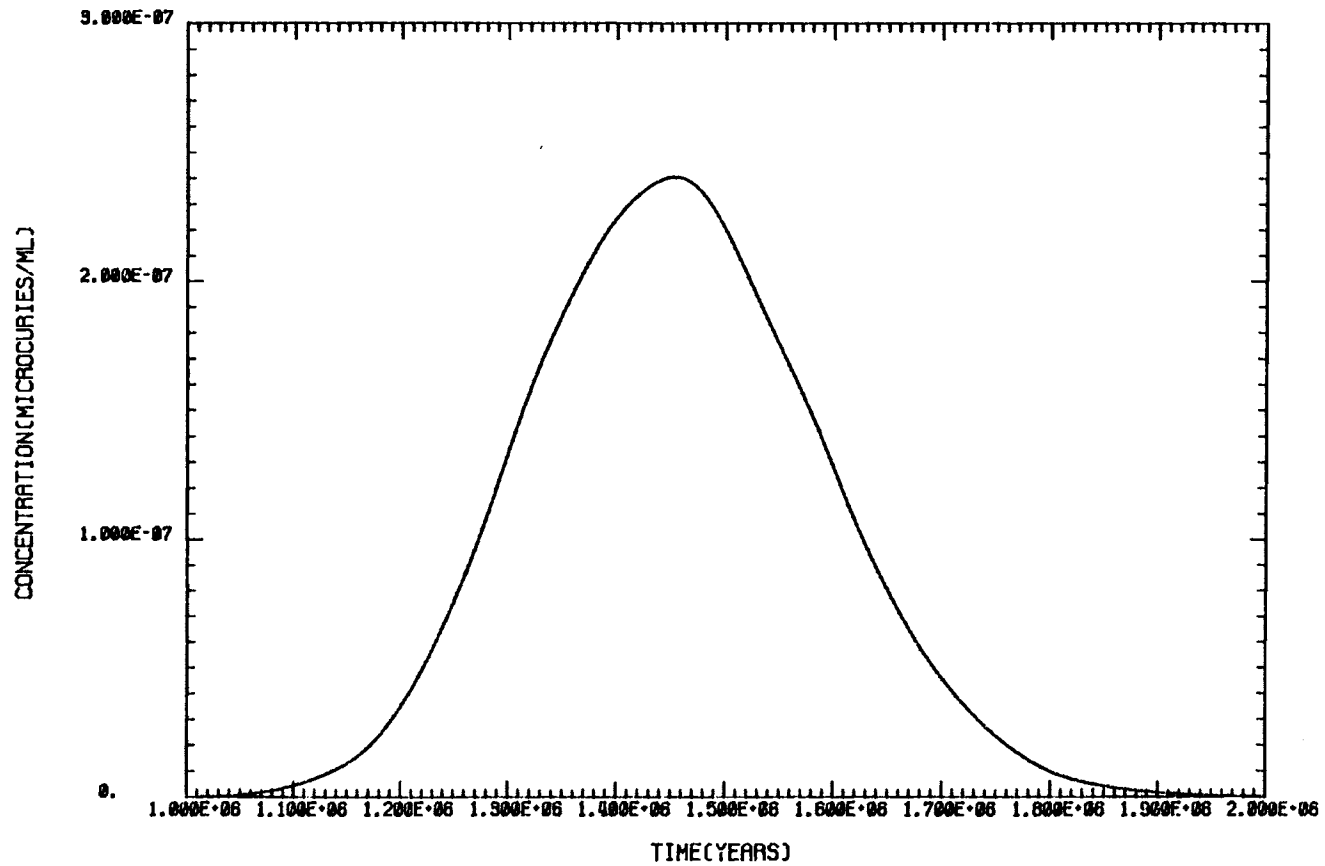


FIGURE 23. WISAP Predicted Malaga Bend Arrival Curve for Cs-135

KD= 2100.00 ML/G HALF-LIFE=8.3000E+07 YEARS BETA= 17.9 G/ML
INITIAL INVENTORY=3.6910E-09 CURIES. PRESENT INVENTORY=7.4634E-10 CURIES.
ISOTOPE PU-244 FLOW TUBE 1 CONCENTRATION VS TIME

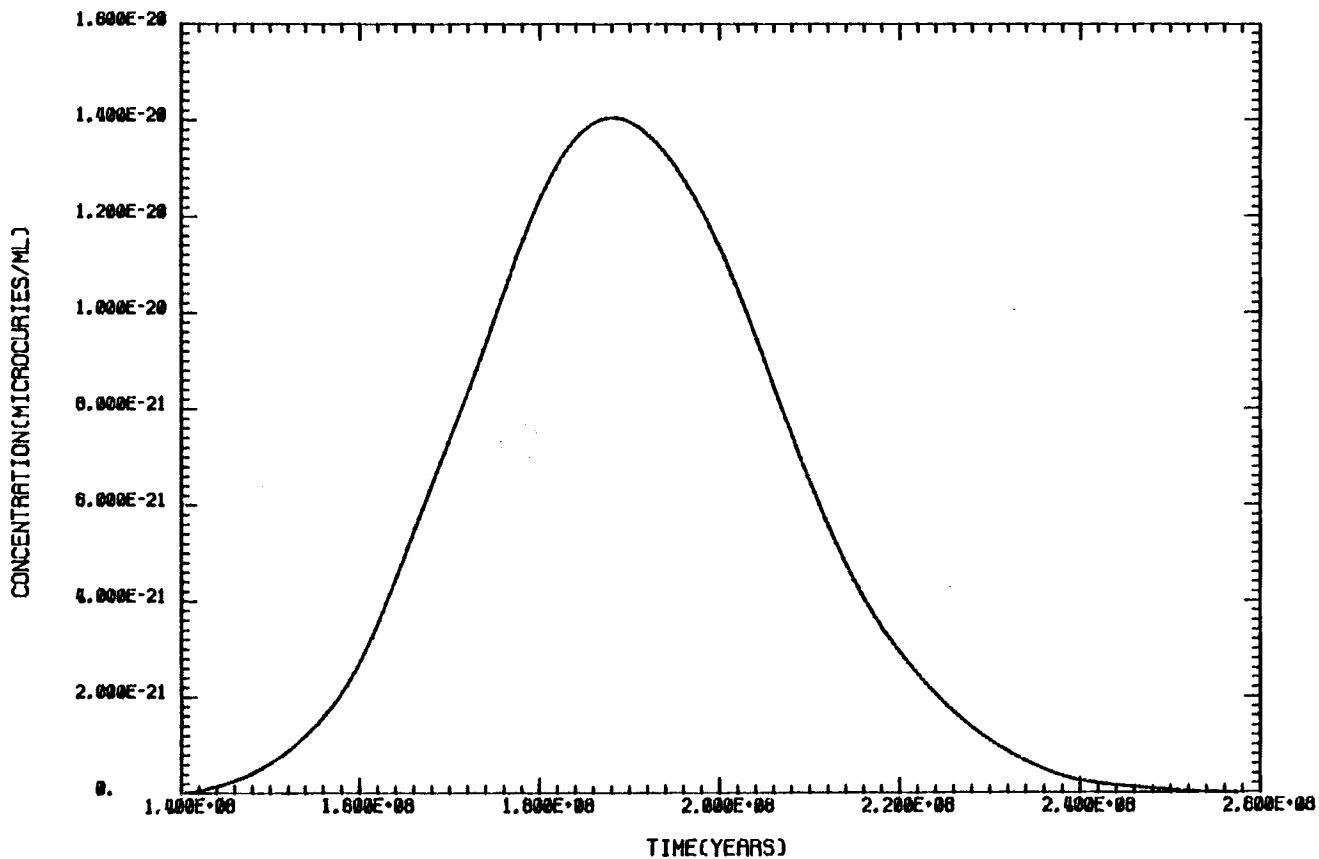


FIGURE 24. WISAP Predicted Alaga Bend Arrival Curve for Actinide Chain 1

KD= 2100.00 ML/G HALF-LIFE=6.5400E+03 YEARS BETA= 17.9 G/ML
INITIAL INVENTORY=2.0290E+05 CURIES. PRESENT INVENTORY=4.2872E-10 CURIES.
ISOTOPE PU-240 FLOW TUBE 1 CONCENTRATION VS TIME

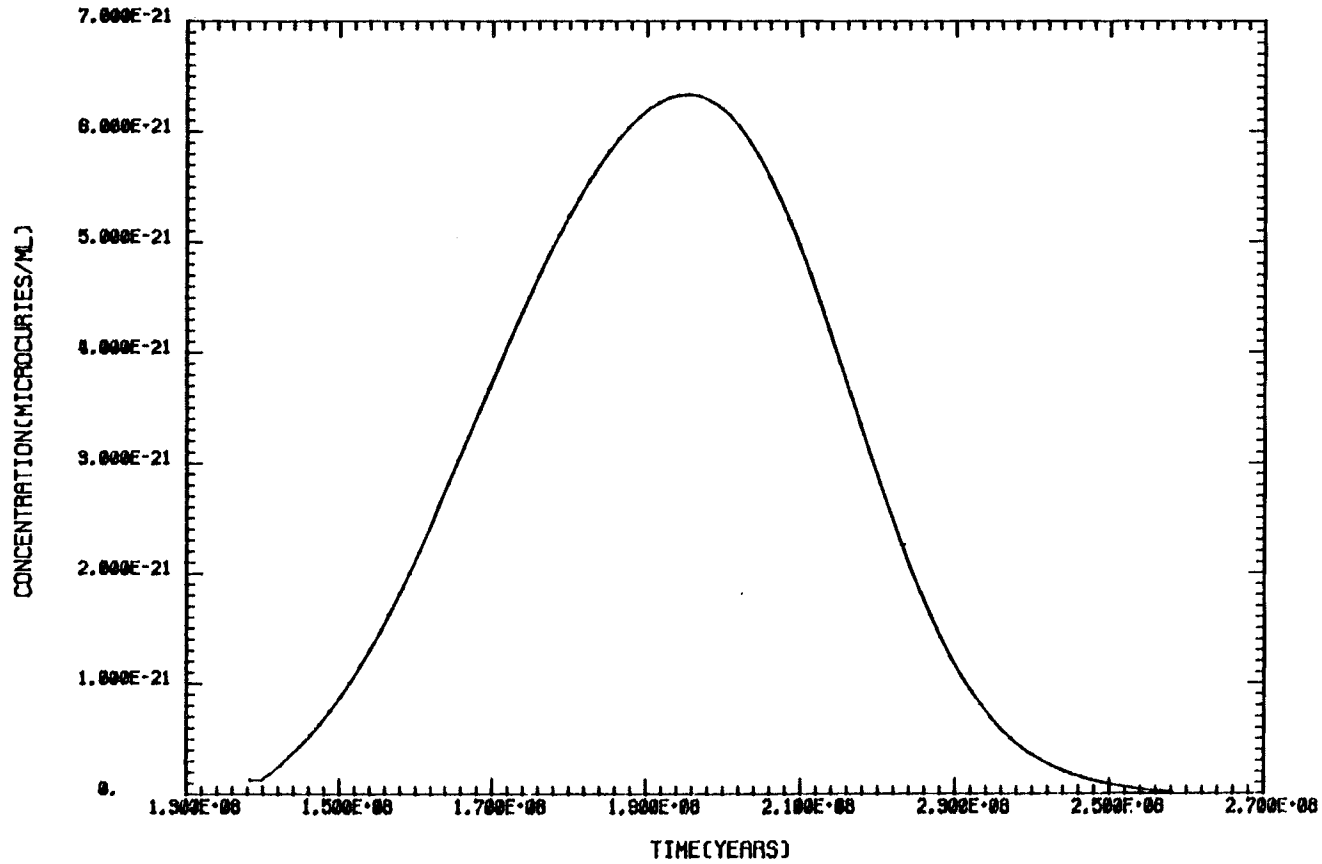


FIGURE 25. WISAP Predicted Malaga Bend Arrival Curve for Actinide Chain 1

KD= 10.00 ML/G HALF-LIFE=2.3400E+07 YEARS BETA= 17.3 G/ML
INITIAL INVENTORY=1.4000E+02 CURIES. PRESENT INVENTORY=1.9097E+02 CURIES.
ISOTOPE U-236 FLOW TUBE 1 CONCENTRATION VS TIME

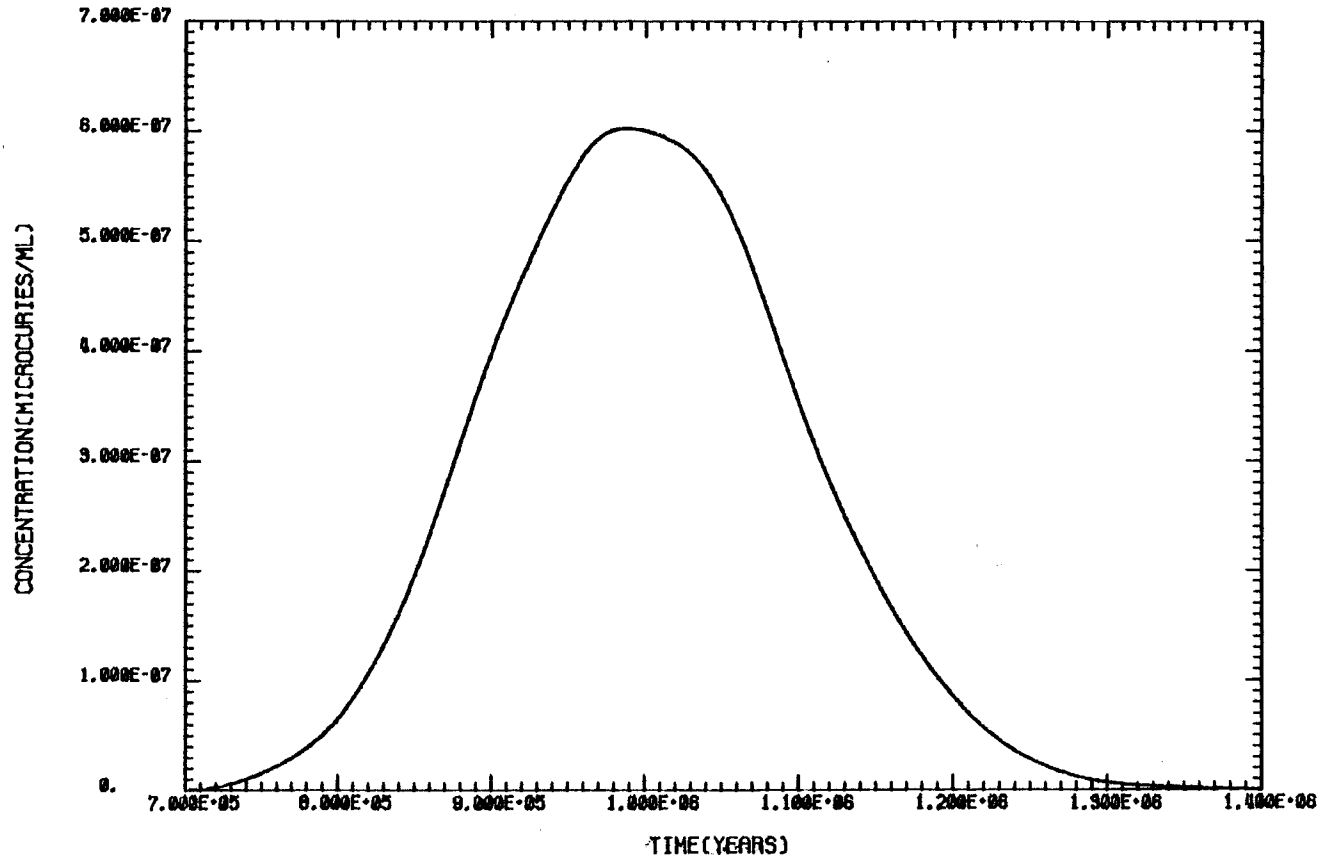


FIGURE 26. WISAP Predicted Malaga Bend Arrival for Actinide Chain 1

KD= 2200.00 ML/G HALF-LIFE=1.4000E+10 YEARS BETA= 17.3 G/ML
INITIAL INVENTORY=6.6840E-06 CURIES. PRESENT INVENTORY=9.5470E-03 CURIES.
ISOTOPE TH-232 FLOW TUBE 1 CONCENTRATION VS TIME

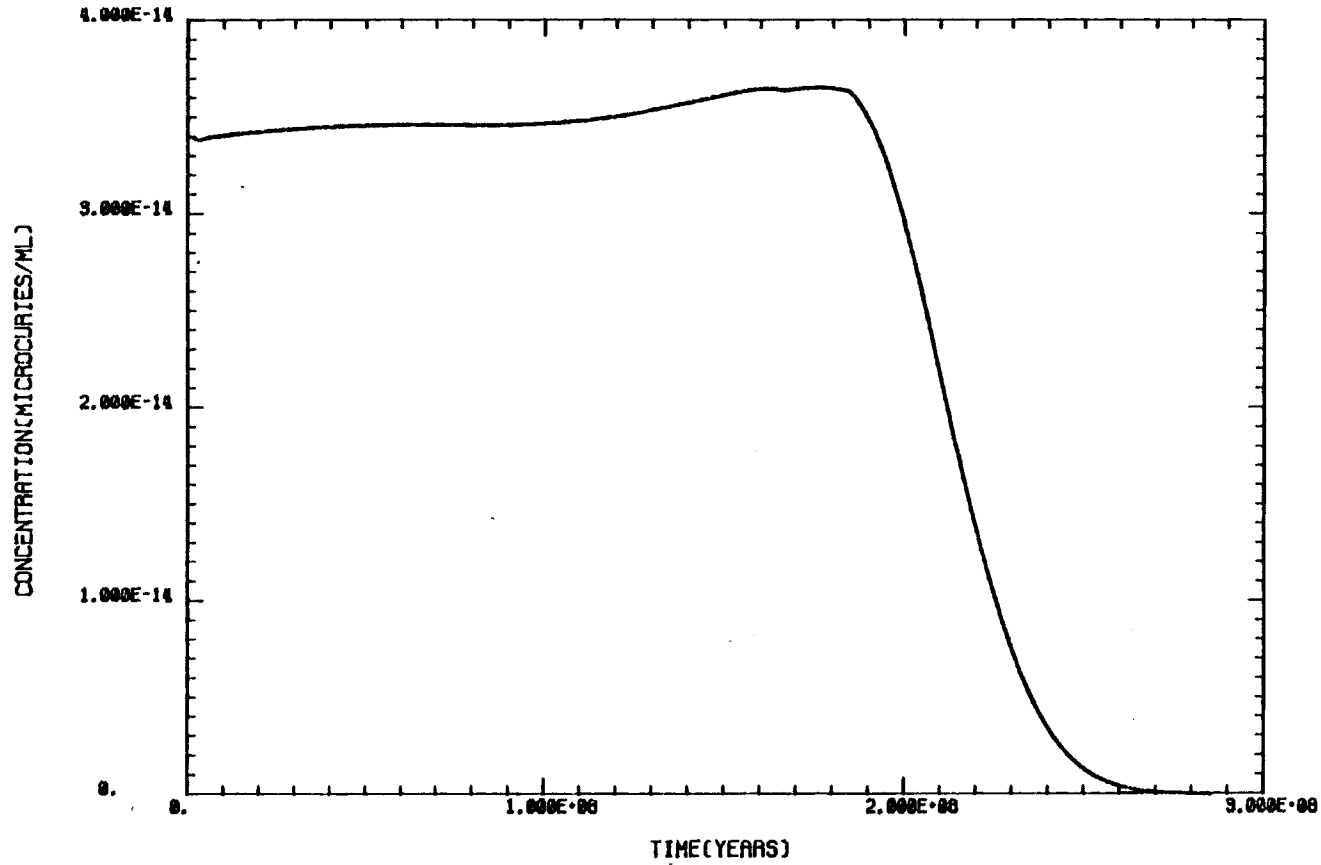


FIGURE 27. WISAP Predicted Malaga Bend Arrival for Actinide Chain 1

KD= 10.00 ML/G HALF-LIFE=1.5800E+05 YEARS BETA= 17.3 G/ML
INITIAL INVENTORY=2.1970E+02 CURIES. PRESENT INVENTORY=1.3177E+02 CURIES.
ISOTOPE U-233 NO. TUBES 1 CONCENTRATION VS TIME

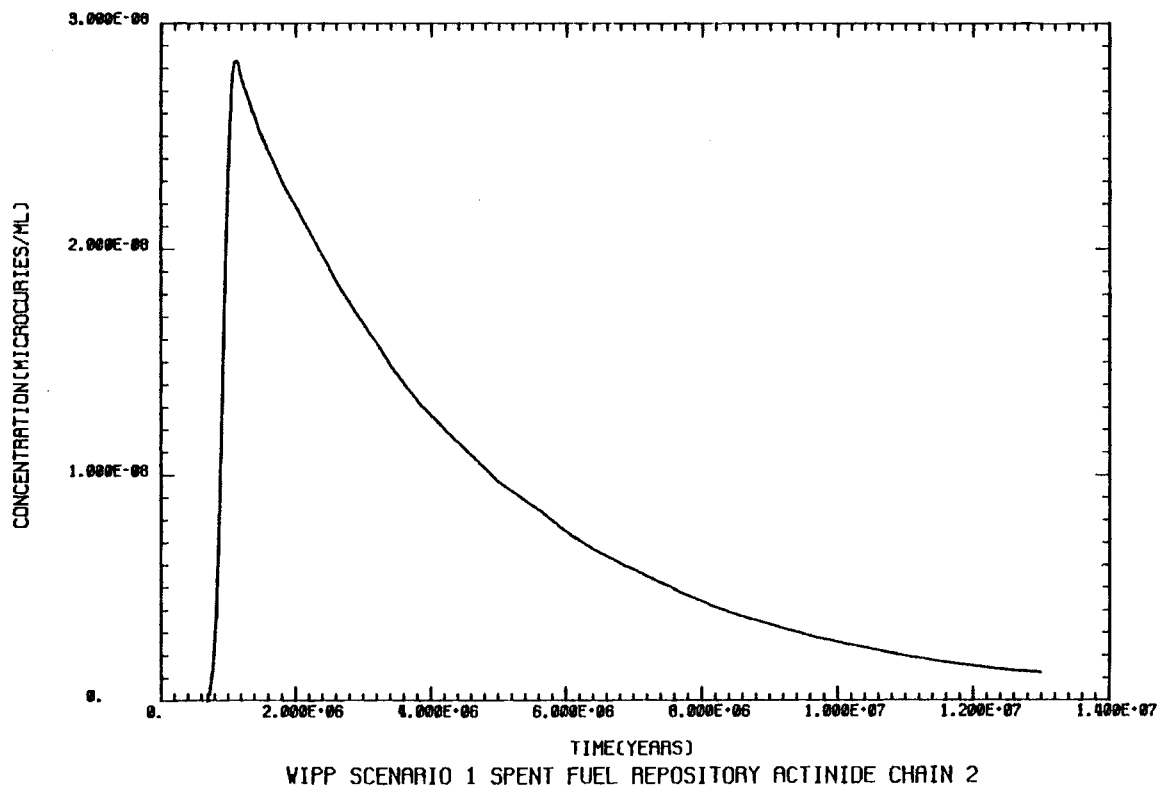


FIGURE 28. WISAP Predicted Malaga Bend Arrival for Actinide Chain 2

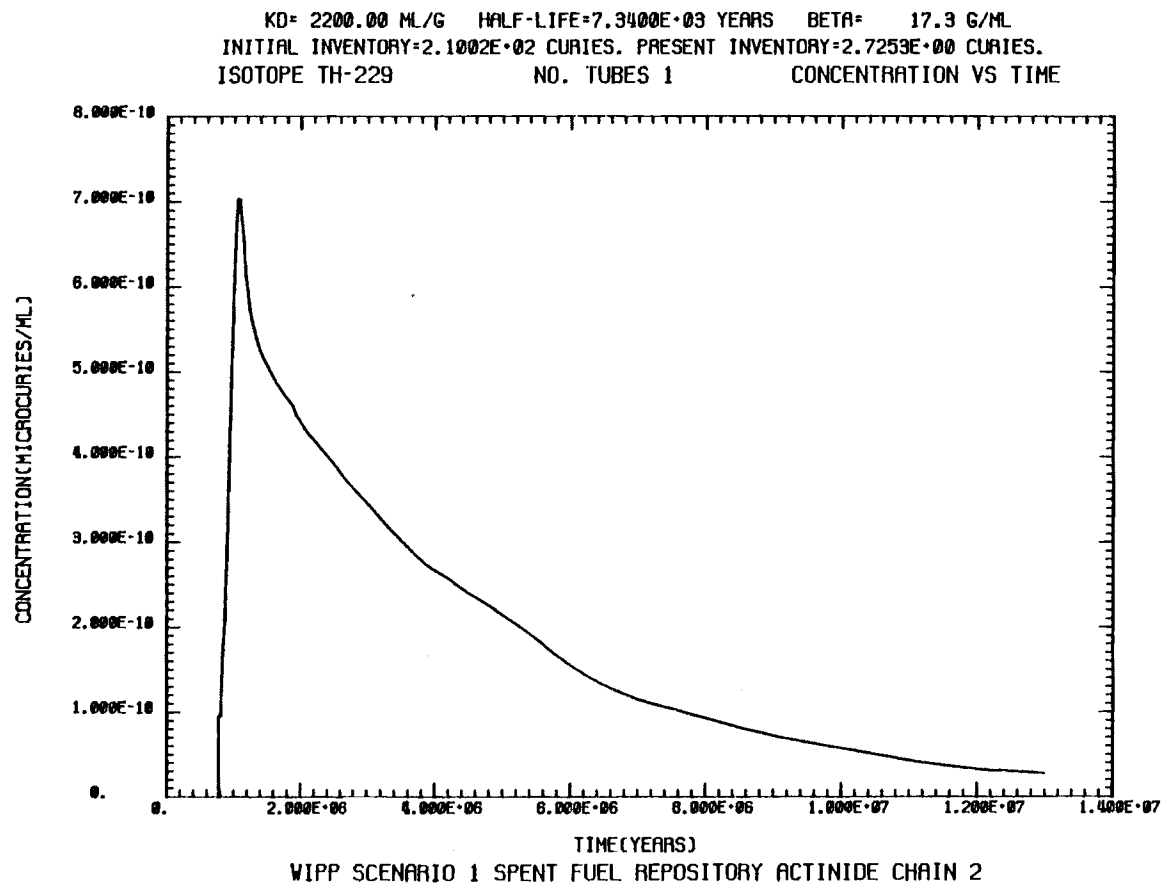


FIGURE 29. WISAP Predicted Malaga Bend Arrival for Actinide Chain 2

KD= 10.00 ML/G HALF-LIFE=4.4700E+09 YEARS BETA= 17.3 G/ML
INITIAL INVENTORY=1.4340E+02 CURIES. PRESENT INVENTORY=1.4341E+02 CURIES.
ISOTOPE U-238 FLOW TUBE 1 CONCENTRATION VS TIME

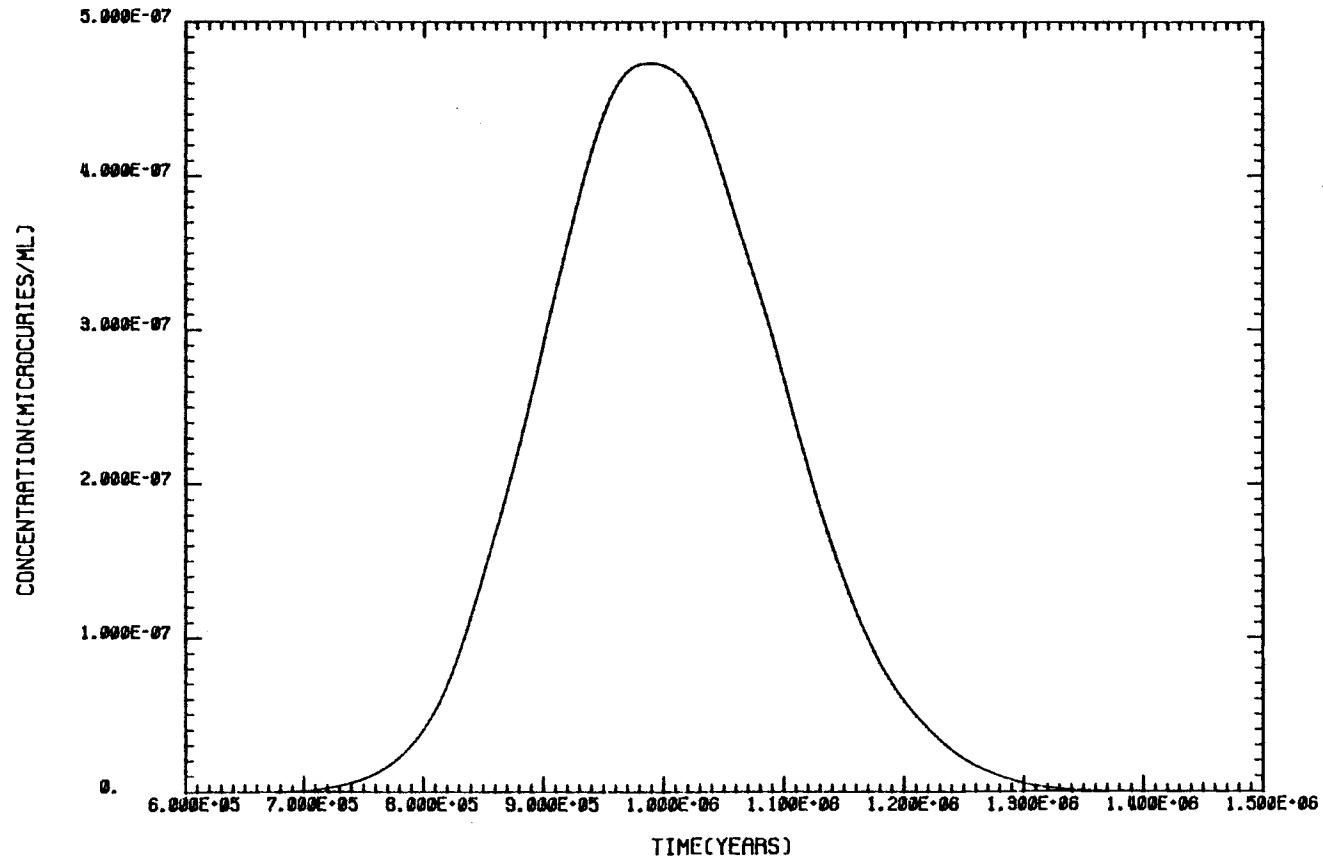


FIGURE 30. Malaga Bend Arrival for Actinide Chain 3

KD= 10.00 ML/G HALF-LIFE=2.4400E+05 YEARS BETA= 17.9 G/ML
INITIAL INVENTORY=8.8690E+02 CURIES. PRESENT INVENTORY=1.8827E+02 CURIES.
ISOTOPE U-234 FLOW TUBE 1 CONCENTRATION VS TIME

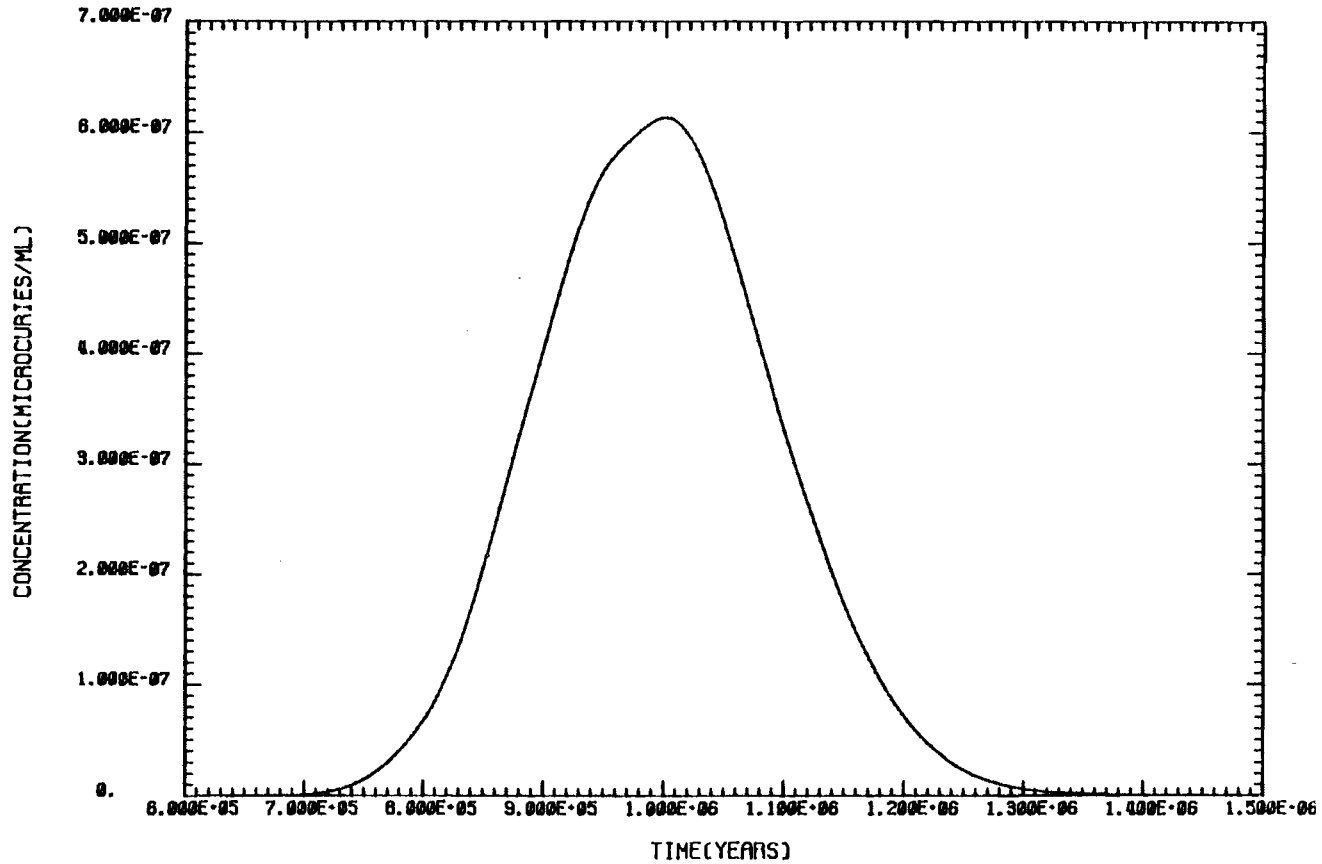


FIGURE 31. WISAP Predicted Malaga Bend Arrival for Actinide Chain 3

KD= 2200.00 ML/G HALF-LIFE=7.7000E+04 YEARS BETA= 17.3 G/ML
INITIAL INVENTORY=6.9260E+00 CURIES. PRESENT INVENTORY=2.2954E+00 CURIES.
ISOTOPE TH-230 FLOW TUBE 1 CONCENTRATION VS TIME

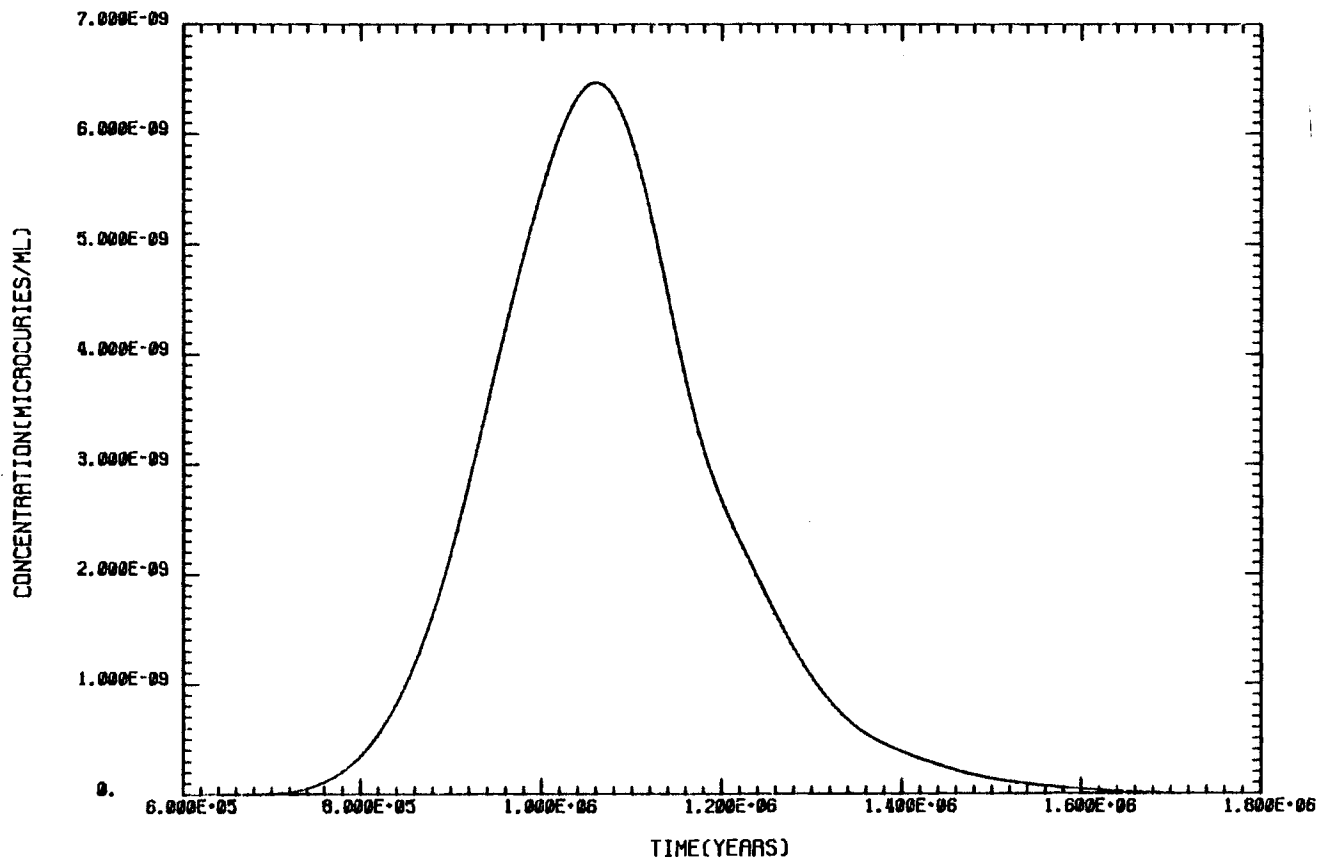


FIGURE 32. WISAP Predicted Malaga Bend Arrival for Actinide Chain 3

KD= 25.00 ML/G HALF-LIFE=1.6000E+03 YEARS BETA= 17.3 G/ML
INITIAL INVENTORY=1.2496E+00 CURIES. PRESENT INVENTORY=5.8243E+01 CURIES.
ISOTOPE RA-226 FLOW TUBE 1 CONCENTRATION VS TIME

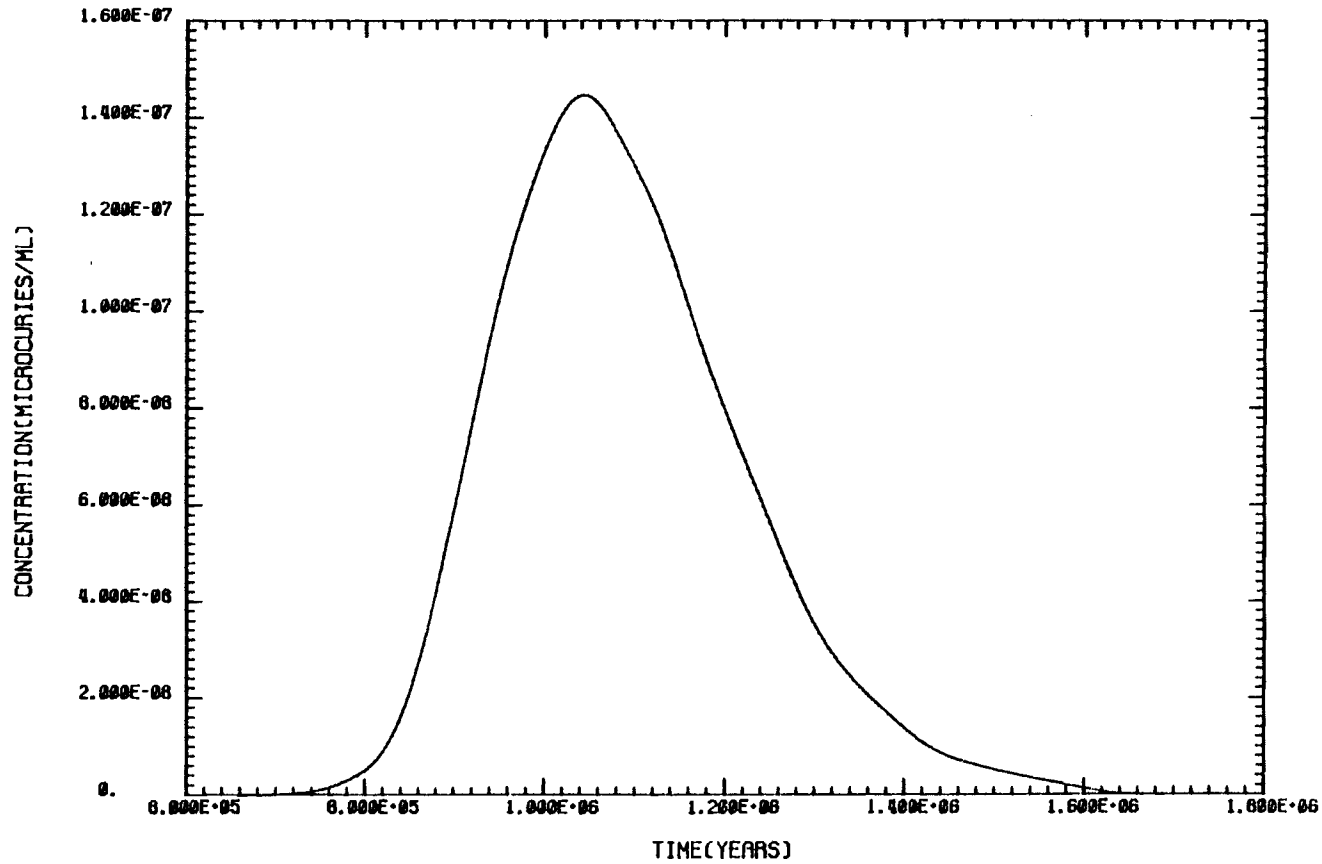


FIGURE 33. WISAP Predicted Malaga Bend Arrival for Actinide Chain 3

KD= 10.00 ML/G HALF-LIFE=7.0400E+08 YEARS BETA= 17.3 G/ML
INITIAL INVENTORY=7.7492E+00 CURIES. PRESENT INVENTORY=1.2923E+01 CURIES.
ISOTOPE U-235 FLOW TUBE 1 CONCENTRATION VS TIME

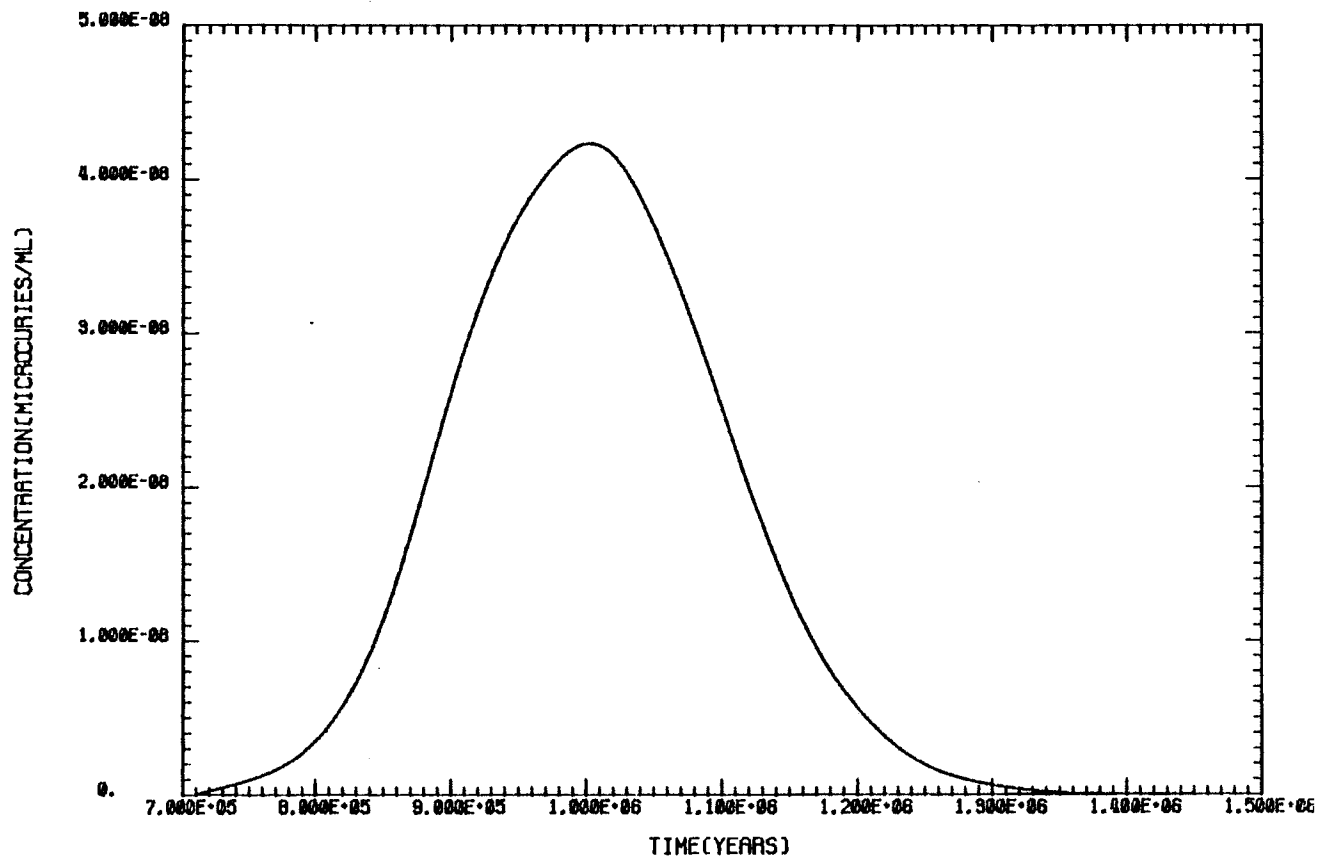


FIGURE 34. WISAP Predicted Malaga Bend Arrival for Actinide Chain 4

KD= 10.00 ML/G HALF-LIFE=9.2500E+04 YEARS BETA= 17.3 G/ML
INITIAL INVENTORY=0.0000E+01 CURIES. PRESENT INVENTORY=1.2795E+01 CURIES.
ISOTOPE PA-231 FLOW TUBE 1 CONCENTRATION VS TIME

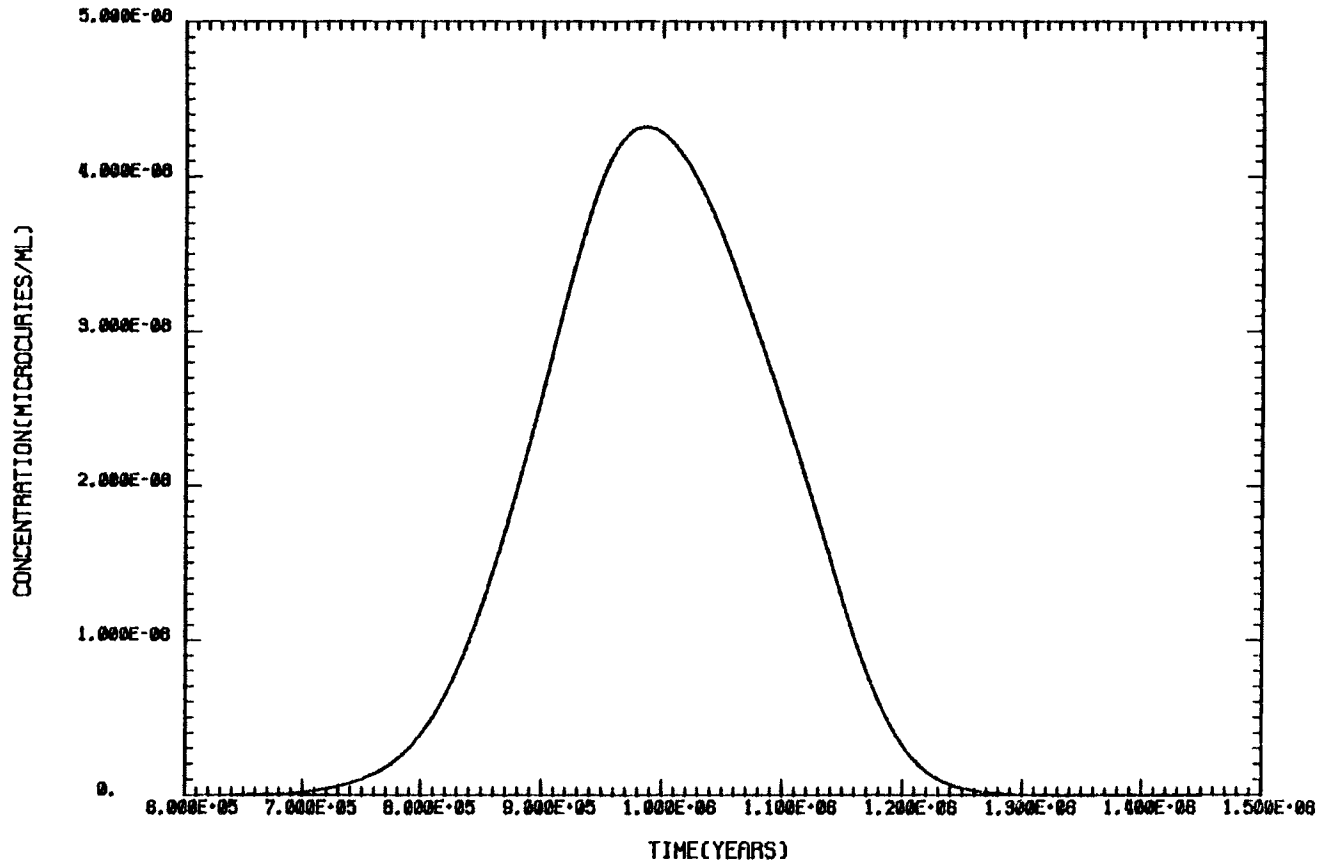


FIGURE 35. WISAP Predicted Malaga Bend Arrival for Actinide Chain 4

TABLE 9. Summary of the WISAP Transport Model Results for Malaga Bend Arrival

ISOTOPE	TOTAL	RELEASE PERIOD		TIME OF PEAK RELEASE (YEARS)	MAXIMUM RATE OF RELEASE TO BIOSPHERE (CURIES/ YEAR)	MAXIMUM CONCEN- TRATION IN GROUND WATER (MICRO- CURIES/ ML)	RATIO OF GROUND WATER CONCEN- TRATION TO MPC**	MAXIMUM CONCEN- TRATION IN THE BIOSPHERE (MICRO- CURIES/ ML)	RATIO OF BIOSPHERE RIVER CONCEN- TRATION TO MPC**
	RELEASED TO BIOSPHERE	MINIMUM TIME	MAXIMUM TIME						
99-TC	5.02E+03	4.38E+03	1.70E+05	8.70E+03	3.97E-02	3.16E-05	1.05E-01	1.71E-06	5.70E-03
129-I	1.49E+01	4.38E+03	1.70E+05	8.70E+03	9.28E-05	7.39E-08	1.23E+00*	4.00E-09	6.66E-02
135-CS	1.01E+02	1.01E+06	2.00E+06	1.45E+06	3.02E-04	2.41E-07	2.41E-03	1.30E-08	1.30E-04
244-PU	7.46E-10	1.41E+08	2.57E+08	1.88E+08	1.76E-17	1.41E-20	3.52E-15	7.58E-22	1.90E-16
240-PU	4.29E-10	1.39E+08	2.60E+08	1.95E+08	7.96E-18	6.34E-21	1.27E-15	3.43E-22	6.86E-17
236-U	1.91E+02	7.02E+05	2.58E+08	9.88E+05	7.57E-04	6.03E-07	2.01E-02	3.26E-08	1.09E-03
232-TH	9.55E-03	7.66E+05	2.85E+08	1.76E+08	4.59E-11	3.65E-14	1.83E-08	1.98E-15	9.89E-10
237-NP	-----	-----	-----	-----	-----	-----	-----	-----	-----
233-U	1.40E+02	7.68E+05	3.33E+07	1.12E+06	3.56E-05	2.83E-08	9.43E-04	1.53E-09	5.11E-05
229-TH	2.80E+00	7.68E+05	3.33E+07	1.12E+06	8.80E-07	7.10E-10	1.01E-04	3.79E-11	5.42E-06
242-PU	-----	-----	-----	-----	-----	-----	-----	-----	-----
238-U	1.43E+02	6.75E+05	3.30E+07	9.86E+05	5.94E-04	4.73E-07	1.16E-02	2.56E-08	6.40E-04
234-U	1.89E+02	6.34E+05	3.30E+07	9.99E+05	7.70E-04	6.13E-07	2.04E-02	3.92E-08	1.11E-03
230-TH	2.30E+00	6.46E+05	3.30E+07	1.06E+06	8.12E-06	6.47E-07	3.23E-01	3.50E-10	1.75E-04
226-RA	6.20E+01	6.59E+05	3.30E+07	1.04E+06	1.82E-04	1.45E-07	4.83E+00*	7.84E-09	2.61E-01
243-AM	-----	-----	-----	-----	-----	-----	-----	-----	-----
239-PU	-----	-----	-----	-----	-----	-----	-----	-----	-----
235-U	1.29E+01	7.11E+05	3.51E+06	1.00E+06	5.31E-05	4.23E-08	1.41E-03	2.29E-09	7.63E-05
231-PA	1.28E+01	6.38E+05	3.44E+06	1.00E+06	5.40E-05	4.32E-08	4.80E-02	2.33E-09	2.59E-03

* INDICATES THAT THE ISOTOPE IS ABOVE MPC.
 ** MPC MAXIMUM PERMISSIBLE WATER CONCENTRATION
 UNCONTROLLED WATER RADIATION STANDARD (MICRO-CI/ML).
 ----- INDICATES THAT THE ISOTOPE DECAYED BEFORE REACHING BIOSPHERE.

REFERENCES

- Waste Isolation Pilot Plant EIS/ER. 1979. Chapter 2, Sections 2.4 through 2.5, Chapter 10, Sections 10.1 through 10.4. U.S. Department of Energy, Washington, D.C.
- Powers, D. W., S. J. Lambert, S. E. Shaffer, L. R. Hill, and W. D. Weart. Editors. 1978. Site Characterization Report for the Waste Isolation Pilot Plant (WIPP), Southeastern New Mexico, Volume 1, SAND-78-1596, Sandia Laboratories, Albuquerque, New Mexico.
- U.S. Energy Research and Development Administration. 1975. "Standards for Radiation Protection," ERDA Manual, Chapter 0524, (Appendix) Annex A, Table II, Column 2.

DISTRIBUTION LIST

<u>No. of Copies</u>		<u>No. of Copies</u>	
	<u>OFFSITE</u>		J. E. Campbell Div. 54.3 Sandia Laboratories Albuquerque, NM 87115
	A. A. Churm DOE Patent Division 9800 South Cass Avenue Argonne, IL 60439	20	Wayne A. Carbiener Office of Nuclear Waste Isolation Battelle Memorial Institute 505 King Avenue Columbus, OH 43201
27	DOE Technical Information Center		H. C. Claiborne Union Carbide Corp. P.O. Box Y Oak Ridge, TN 39380
2	Argonne National Laboratory Reference Library 9800 South Cass Avenue Argonne, IL 60439		Neville G. W. Cook Department of Materials Science and Mineral Engineering Hearst Mining Building University of California Berkeley, CA 94720
	G. E. Barr Div. 1141 Sandia Laboratories Albuquerque, NM 87115		Carl R. Cooley DOE Office of Nuclear Waste Management Washington, DC 20545
	Battelle Memorial Institute Office of Nuclear Waste Isolation Attn: Beverly Rawles 505 King Avenue Columbus, OH 43201		Jared Davis Nuclear Regulatory Commission Washington, DC 20555
	John Bird Geology Department Cornell University Ithaca, NY 14853		George DeBuchananne U.S. Geological Survey Reston, VA 22092
	J. D. Bredehoeft U.S. Geological Survey Water Resources Division Reston, VA 22092		R. T. Dillon Div. 5413 Sandia Laboratories Albuquerque, NM 87115
2	Brookhaven National Laboratory Reference Section Information Division Upton, Long Island, NY 11973		

No. of
Copies

No. of
Copies

J. O. Duguid
Office of Nuclear Waste
Isolation
Battelle Memorial Institute
505 King Avenue
Columbus, OH 43201

Environmental Protection Agency
Office of Radiation Programs
Technical Assessment Division
AW559
Washington, DC 20460

Robert M. Garrells
Department of Geologic Sciences
Northwestern University
Evanston, IL 60201

Geraghty & Miller, Inc.
44 Sintsink Dr. East
Port Washington, NY 11050

W. G. Gray
Department of Civil
Engineering
Princeton University
Princeton, NJ 08540

D. B. Grove
U.S. Geological Survey
WRD
Mail Stop 413
Denver Federal Center
Denver, CO 80225

John Handin, Director
Center for Tectomophysics
Texas A M University
College Station, TX 77840

Colin A. Heath
DOE Office of Nuclear Waste
Management
Washington, DC 20545

William M. Hewitt
Office of Nuclear Waste
Isolation
Battelle Memorial Institute
505 King Avenue
Columbus, OH 43201

Peter L. Hofmann
Office of Nuclear Waste
Isolation
Battelle Memorial Institute
505 King Avenue
Columbus, OH 43201

Muzaffer Kehnemuyi
Office of Nuclear Waste
Isolation
Battelle Memorial Institute
505 King Avenue
Columbus, OH 43201

John F. Kircher
Office of Nuclear Waste
Isolation
Battelle Memorial Institute
505 King Avenue
Columbus, OH 43201

Ronald B. Lantz
Inter-Environmental Consultants
11511 Katy Freeway
Houston, TX 77079

2 Lawrence Berkeley Laboratory
Reference Library
University of California
Berkeley, CA 94720

2 Lawrence Livermore Laboratory
Reference Library
P.O. Box 808
Livermore, CA 94550

D. I. Leap
U.S. Geological Survey
Water Resources Division
MS 416
Denver Federal Center
Denver, CO 80225

No. of
Copies

No. of
Copies

	S. E. Logan Los Alamos Technical P.O. Box 410 Los Alamos, NM 87544	2	Barry Naft NUS Corporation 4 Research Place Rockville, MD 20805
2	Los Alamos Scientific Laboratory Reference Library P.O. Box 1663 Los Alamos, NM 87544		T. N. Narasimhan Lawrence Berkeley Laboratory Berkeley, CA 94720
	John Lyons Department of Earth Sciences Dartmouth College Hanover, NH 03755	2	J. O. Neff Department of Energy Columbus Program Office 505 King Avenue Columbus, OH 43201
	R. D. MacNish U.S. Geological Survey Water Resources Div. 301 West Congress Tucson, AR 85701	2	Neil A. Norman Environmental Sciences Department Bechtel National Inc. P.O. Box 3965 San Francisco, CA 94105
	J. B. Martin Asst. Director for Radioactive Waste Management Branch NRC Division of Materials and Fuel Cycle Facility Licensing Washington, DC 20555	2	Oak Ridge National Laboratory Central Research Library Document Reference Section Oak Ridge, TN 37830
	John T. McGinnis Office of Nuclear Waste Isolation Battelle Memorial Institute 505 King Avenue Columbus, OH 43201		Frank L. Parker Department of Environmental Engineering Vanderbilt University Nashville, TN 37235
	Sheldon Meyers DOE Office of Nuclear Waste Management Washington, DC 20545		L. W. Picking Stone & Webster Engineering Corporation 245 Summer Street Boston, MA 02107
	P. A. Mote Bechtel National, Inc. 50 Beale Street San Francisco, CA 94119		George Pinder Department of Civil Engineering Princeton University Princeton, NJ 08540

No. of
Copies

Gary Robbins
U.S. Nuclear Regulatory
Commission
Division of Waste Management
Washington, DC 20555

2 Savannah River Laboratory
Reference Library
Aiken, SC 29801

G. Segol
Bechtel National, Inc.
50 Beale Street
San Francisco, CA 94119

Raymond Siever
Department of Geological
Sciences
Harvard University
Cambridge, MA 02138

Howard P. Stephens
Sandia Laboratories
P.O. Box 5800
Albuquerque, NM 87115

David B. Stewart
U.S. Geological Survey
National Center 959
Reston, VA 22092

Lewis D. Thorson
Lawrence Livermore Laboratory
Box 803, L-224
Livermore, CA 94550

N. P. Timofeef
State University of New York
Binghamton, NY 13901

Wendal Weart
Division 1140
Sandia Laboratories
Albuquerque, NM 87115

No. of
Copies

Robert Williams
Electric Power Research
Institute
P.O. Box 10412
Palo Alto, CA 94304

Paul A. Witherspoon
Lawrence Berkeley Laboratory
University of California
Berkeley, CA 94710

FOREIGN

D'Allessandro Avogadro
Commission of European
Communities
Joint Research Centre
I-21020 Ispra (Varese)
ITALY

V. K. Barwell
Environmental Research Branch
Atomic Energy of Canada Limited
Chack River, Ontario KOJ1J0
CANADA

Bundesministerium fur Forschung
und Technologie
Stressemanstrasse 2
D-5300 Bonn
F.R. of GERMANY

J. A. Cherry
Department of Earth Sciences
Waterloo, Ontario
CANADA

Center for Atomic Energy
Documentation (ZAED)
ATTN: Dr. Bell
Postfach 3640
D-7500 Karlsruhe
F.R. of GERMANY

No. of
Copies

Ferruccio Gera
Radiation Protection and
Waste Management Division
Nuclear Energy Agency/OECD
38 boulevard Suchet
75016 Paris
FRANCE

2 INIS Clearinghouse
International Atomic Energy
Agency
P.O. Box 590
A-1011, Vienna
AUSTRIA

Klaus Kuhn
Institut für Tiefagerung
Wissenschaftliche Abteilung
Berliner Strasse 2
D-3392 Clausthal - Zellerfeld
F.R. of GERMANY

Hans W. Levi
Hahn-Meitner-Institut für
Kernforschung
Glienicke Strasse 100
D-1000 Berlin 39
F.R. of GERMANY

Library
Studsvik Energiteknik AB
S-611 01 Nyköping
SWEDEN

Franz Peter Oesterle
Physikalisch-Chemische
Bundesanstalt
Bundesallee 100
D-3300 Braunschweig
F.R. of GERMANY

Toñis Papp
Kärnbränslesäkerhet
Fack. 10240
Stockholm
SWEDEN

No. of
Copies

T. Vandergraff
Atomic Energy of Canada Limited
Whiteshell Nuclear Research
Establishment
Pinawa, Manitoba ROE 1LQ
CANADA

Egbert Schapermeier
Battelle-Institute e.V.
Am Romerhof 35
D-6000 Frankfurt am Main 90
F.R. of GERMANY

ONSITE

4 DOE Richland Operations Office
O. J. Elgert
H. E. Ransom
J. J. Schreiber
F. R. Standerfer

6. Rockwell Hanford Operations
R. C. Arnett
R. G. Baca
R. L. Bielefeld
D. J. Carrell
R. A. Deju
Rockwell Document Control

62 Pacific Northwest Laboratory
G. L. Benson
D. L. Bradley
A. Brandstetter (10)
F. W. Bond (5)
S. M. Brown
D. B. Cearlock
M. O. Cloninger
C. R. Cole (10)
F. H. Dove
D. R. Friedrichs
S. R. Gupta
M. A. Harwell
B. W. Howes

No. of
Copies

J. H. Jarrett
F. E. Kaszeta
M. R. Kreiter
R. W. Nelson
A. M. Platt
A. E. Reisenauer
R. J. Serne
D. J. Silviera

No. of
Copies

C. S. Simmons
J. K. Soldat
J. F. Washburn
Technical Information Library
(5)
Publishing Coordination R0(2)
Water and Land Resources
Department Library (10)